JGR Atmospheres

RESEARCH ARTICLE
10.1029/2020JD032974

The Vulcan Version 3.0 High-Resolution Fossil Fuel CO_2 Emissions for the United States

Kevin R. Gurney[1], Jianming Liang[2,3], Risa Patarasuk[2,4], Yang Song[2], Jianhua Huang[2,5], and Geoffrey Roest[1]

[1]School of Informatics, Computing, and Cyber Systems, Northern Arizona University, Flagstaff, AZ, USA, [2]School of Life Sciences, Arizona State University, Tempe, AZ, USA, [3]ESRI, Redlands, CA, USA, [4]Citrus County Board of Commissioners, Lecanto, FL, USA, [5]VISA Research, Austin, TX, USA

Key Points:
- Vulcan v3.0 is the first U.S.-wide bottom-up $FFCO_2$ emissions data product at 1 km^2/hourly for multiple years
- Comparison to satellite-driven global $FFCO_2$ emissions shows large spatial differences with a mean gridcell absolute relative difference of 104.3%
- Vulcan can provide an immediate Scope 1 $FFCO_2$ inventory for every city in the United States saving city time and resources

Supporting Information:
- Supporting Information S1

Correspondence to:
K. R. Gurney,
kevin.gurney@nau.edu

Citation:
Gurney, K. R., Liang, J., Patarasuk, R., Song, Y., Huang, J., & Roest, G. (2020). The Vulcan version 3.0 high-resolution fossil fuel CO_2 emissions for the United States. *Journal of Geophysical Research: Atmospheres*, *125*, e2020JD032974. https://doi.org/10.1029/2020JD032974

Received 6 MAY 2020
Accepted 30 AUG 2020
Accepted article online 15 SEP 2020

Abstract Estimates of high-resolution greenhouse gas (GHG) emissions have become a critical component of climate change research and an aid to decision makers considering GHG mitigation opportunities. The "Vulcan Project" is an effort to estimate bottom-up carbon dioxide emissions from fossil fuel combustion and cement production ($FFCO_2$) for the U.S. landscape at space and time scales that satisfy both scientific and policy needs. Here, we report on the Vulcan version 3.0 which quantifies emissions at a resolution of 1 km^2/hr for the 2010–2015 time period. We estimate 2011 $FFCO_2$ emissions of 1,589.9 TgC with a 95% confidence interval of 1,367/1,853 TgC (−14.0%/+16.6%), implying a one-sigma uncertainty of ~ ±8%. Per capita emissions are larger in states dominated by electricity production and industrial activity and smaller where onroad and building emissions dominate. The U.S. $FFCO_2$ emissions center of mass (CoM) is located in the state of Missouri with mean seasonality that moves on a near-elliptical NE/SW path. Comparison to ODIAC, a global gridded $FFCO_2$ emissions estimate, shows large total emissions differences (100.4 TgC for year 2011), a spatial correlation of 0.68 (R^2), and a mean absolute relative difference at the 1 km^2 scale of 104.3%. The Vulcan data product offers a high-resolution estimate of $FFCO_2$ emissions in every U.S. city, obviating costly development of self-reported urban inventories. The Vulcan v3.0 annual gridded emissions data product can be downloaded from the Oak Ridge National Laboratory Distributed Active Archive Center (Gurney, Liang, et al., 2019, https://doi.org/10.3334/ORNLDAAC/1741).

Plain Language Summary The emission of greenhouse gases into the Earth atmosphere is driving climate change. The largest single emission category is the release of carbon dioxide from the combustion of fossil fuels. Cities account for roughly 70% of the global emissions of fossil fuel carbon dioxide. Understanding where and when these emissions occur is critical to the science of climate change and to guiding the steps needed to lower these emissions. The Vulcan version 3.0 fossil fuel carbon dioxide emissions data product quantifies all of these emissions for the entire U.S. domain at spatial scales of 1 km^2 for every hour from the years 2010–2015. It is constructed from a large number of publicly available data sources such as pollution reporting, energy statistics, powerplant stack monitoring, and traffic counts. This data product is freely available for scientific research and policy guidance purposes and offers insights, understanding, and application to practical questions.

1. Introduction

Global emissions of carbon dioxide from the combustion of fossil fuels ($FFCO_2$) comprise the largest net flux of carbon into the Earth's atmosphere and remain the primary driver of anthropogenic climate change (Intergovernmental Panel on Climate Change, 2013; USGCRP, 2018). Improving our quantitative understanding of $FFCO_2$ fluxes remains a critical component of climate change research and climate policy. For example, scientific understanding of the global carbon cycle and how it interacts with climate change rests on accurate quantification of $FFCO_2$ emissions at multiple scales (LeQuéré et al., 2018). This, in turn, improves the reliability of future projections of climate change and specifies the emissions reductions necessary to meet specific targets, such as limiting the rise of global mean temperature to 1.5°C (IPCC, 2018). Understanding $FFCO_2$ sources also assists in understanding the composition, driving factors, and responsibility for emissions, making mitigation options better targeted, equitable, and ultimately more effective (Durant et al., 2011; National Research Council, 2010).

Quantification of $FFCO_2$ emissions began as efforts to capture total emissions at the global and national spatial scales aiming to quantify anthropogenic fluxes to better understand the drivers of climate change and the global carbon cycle (Keeling, 1973). Employing accounting approaches that rely on national statistics of energy production and consumption, a number of national and international institutions produce and archive estimates of $FFCO_2$ emissions, often disaggregated to economic sector and fuel type (see reviews by Andres et al., 2012; Macknick, 2011). In response to the advances in carbon cycle observations and modeling studies, many of these $FFCO_2$ inventory products began to increase their spatial and temporal resolution below the nation state, often representing emissions in regularized gridded format (Andres et al., 1996; Marland et al., 1985; Olivier et al., 1999). Gridded output was especially important when used within systems that solve carbon fluxes through inversion of atmospheric transport constrained by atmospheric concentration measurements (Gaubert et al., 2019; Gurney et al., 2002, 2005; Peylin et al., 2011; Yadav et al., 2016). Most often these subnational representations of $FFCO_2$ emissions used proxy information, such as population statistics and/or remotely sensed nighttime lights, to distribute the national/global emissions to smaller space/time scales (Andres et al., 1999; Ghosh et al., 2010; Oda & Maksyutov, 2011; Olivier et al., 2005; Ou et al., 2015; Rayner et al., 2010). Recent research has employed a mixture of global "bottom-up" information such as powerplant databases with remote sensing information (e.g., Jannsens-Maenhout et al., 2019; Oda et al., 2018; Wang et al., 2013), sometimes within optimization frameworks to more mechanistically distribute emissions in space and time in addition to offering more formal uncertainty estimation (Asefi-Najafabady et al., 2014; Rayner et al., 2010).

In addition to the globally gridded representations, research effort has also aimed at specific national and regional domains often with additional detail on the emitting process (Bun et al., 2007, 2018; Cai et al., 2018; Denier van der Gon et al., 2017; Gately & Hutyra, 2017; Gregg & Andres, 2008; Gregg et al., 2009; Ivanova et al., 2017; Kurokawa et al., 2013) with some studies focused on an individual sector or source type (Danylo et al., 2019; Gately et al., 2013; Liu et al., 2015; Petron et al., 2008; Wang et al., 2014; Zheng et al., 2014). These national and regional efforts were often modeled in a fashion similar to, and inclusive of, local air pollution inventories (Baldasano et al., 2008; Cooke et al., 1999; Hoesly et al., 2018; Ohara et al., 2007). In addition to focusing on different national domains with unique data sets, many of these past research efforts reflect different methodological approaches to data interpretation, downscaling and modeling. Among these efforts is the pioneering work of the Vulcan Project begun in 2004, the first attempt to generate a completely bottom-up space/time-explicit national estimate of all $FFCO_2$ emission sources (Gurney et al., 2009). The Vulcan Project, which estimated $FFCO_2$ emissions at the "native" resolution of emission points, lines, and polygons, originally produced United States (U.S.) $FFCO_2$ emissions on a 10 km × 10 km spatial grid at hourly time resolution for the year 2002. Used in a variety of research and applied policy settings, the Vulcan Project has spawned additional efforts at downscaling into the urban domain, where resolution has gone to the scale of individual buildings and street segments for whole urban areas (Gurney et al., 2012, 2018; Gurney, Patarasuk, et al., 2019; Patarasuk et al., 2016; Pincetl et al., 2014; Shu & Lam Nina, 2011; VandeWeghe & Kennedy, 2007; Wilson et al., 2013; Zhou & Gurney, 2011). In addition to supporting atmospheric CO_2 inversion work at the urban scale, the granular estimates can be used to more efficiently target emissions mitigation policy (Gurney et al., 2015; Lauvaux et al., 2020). Other efforts have been developed since the first release of Vulcan output with similar approaches such as the Anthropogenic Carbon Emissions System (ACES) data product in the northeastern United States (Gately & Hutyra, 2017) and the work of Bun and colleagues in Poland (Bun et al., 2018; Charkovska et al., 2019; Danylo et al., 2019). Though similar in general approach, they offer alternative methodological details and data sources to bottom-up $FFCO_2$ estimation.

In this paper, we introduce version 3.0 of the Vulcan Project estimation of high-resolution U.S. fossil fuel carbon dioxide emissions and CO_2 emissions from cement production (collectively referred to here as "$FFCO_2$"). We report here on the methodology, space/time resolution, and uncertainty estimation. We also present some of the fundamental results of the Vulcan output and compare to the only commensurate resolved $FFCO_2$ emissions data product covering the entire U.S. landscape, the ODIAC global data product. Vulcan is distinct from ODIAC in that it includes detail regarding combustion sector, combustion subsector (e.g., by vehicle class, building type), combustion process (e.g., boiler, turbine, engine), and a detailed fuel characterization (e.g., individual petroleum fuels, coal grade). Though reported here as gridded output, the underlying emissions content is quantified as individual point, line, and polygon source elements and as such, is distinct in potentially providing finer resolution in the future. Finally, unlike top-down

inventories, typically produced at the global scale, Vulcan is constructed from the bottom-up, relying less on indirect spatial proxies (e.g., nighttime lights) and more on detailed mapping of physical entities such as roadways and factories. Finally, we show results associated with a few zoomed urban locations, suggesting that the Vulcan $FFCO_2$ emissions data product has a role to play in providing U.S. cities with a subcity resolved Scope 1 CO_2 emissions inventory.

Version 3.0 of the Vulcan data product and associated documentation is publicly available and annual, gridded, multiyear results can be downloaded from the Oak Ridge National Laboratory Distributed Active Archive Center (ORNL DAAC) (https://doi.org/10.3334/ORNLDAAC/1741).

This paper is structured as follows: In section 2, we describe the input data and model processes used to generate the Vulcan version 3.0 $FFCO_2$ emissions data product including those used for spatial and temporal distribution. In section 3, we present the results, the uncertainties and a series of descriptive statistics at various scales of aggregation. In section 4, we compare Vulcan to the ODIAC data product and discuss the potential use and relevance of this work, known gaps and weaknesses, in addition to next steps and future work.

2. Materials and Methods

The Vulcan version 3.0 $FFCO_2$ emissions data product represents total $FFCO_2$ emissions resulting from the combustion of fossil fuel (coal, petroleum, and natural gas) and CO_2 from cement production in the 50 United States and District of Columbia for 2010–2015 time period (Gurney, Liang, et al., 2019). It is constructed from multiple public data sets that generate emissions magnitude, the spatial representation, and temporal representation of those emissions. The $FFCO_2$ emissions are initially estimated at their "native" spatial and temporal resolution (e.g., counties, points, lines, annual, hourly as opposed to the gridded results) depending upon the characteristics of the incoming data sources. Additional spatial and temporal distribution (e.g., downscaling, interpolation, proxy surrogates), where needed, is used to achieve an hourly representation for six complete calendar years (2010–2015) at the spatial resolutions of a U.S. Census block-group or finer (e.g., points, lines). The $FFCO_2$ emissions are further processed to regularized hourly grids at a resolution of 1 km × 1 km, for the contiguous United States and Alaska. The $FFCO_2$ emissions represent all fossil fuel combustion extending 12 nautical miles from the coastal boundary of the United States and up to 3,000 ft associated with aircraft takeoff/landing procedures.

The Vulcan $FFCO_2$ emissions data product is categorized as "Scope 1" or "in-boundary" emissions. They are an accounting of emissions that reflect physical release of CO_2 molecules from the stated geography (e.g., gridcell, state, province). This is in contrast to quantification of fluxes that assign emissions to consumptive activity such as through the use of electricity or consuming food (Davis & Caldeira, 2010). The two accounting perspectives are identical at the whole-planet scale but diverge as one considers scales at the nation state or below. Consumption-based $FFCO_2$ emissions quantification has a long history at scales ranging from the nation state to the city but has only recently begun to systematically resolve (e.g., in gridded form) $FFCO_2$ emissions below the nation state scale (Jones & Kammen, 2011, 2014; Minx et al., 2013; Moran et al., 2018; Zhang et al., 2014). The current study quantifies in-boundary emissions because these can be directly used with atmospheric monitoring, a critical element in evaluation/validating the estimated fluxes and a motivation for the research reported here (NRC 2010).

2.1. Data and Processing

The data sources for the $FFCO_2$ emissions estimation are organized here by data source type and/or the economic sector in accordance with the original data collection/categorization (see Table 1). Further detail on data sources and references are provided in the sector/type subsections in addition to the supporting information. Though earlier publications have described results of the Vulcan Project, detailed methodological documentation was not included in the peer-reviewed literature. Hence, this paper serves as the complete methodological record of the Vulcan methods (Gurney et al., 2009; Zhou & Gurney, 2011). Uncertainty quantification represents a 95% confidence interval (CI). Due to the considerable runtime of the Vulcan codebase, only the boundaries of the upper and lower CI are estimated (referred to as "hi" and "lo" CI bounds). Details on the uncertainty estimation are included in each of the sector/type subsections. Future versions of the Vulcan data product will quantify a more complete uncertainty distribution of the Vulcan $FFCO_2$ emissions output.

Table 1
Overview of Data Sources Used in Generating the Space/Time-Resolved Vulcan v3.0 $FFCO_2$ Emissions (Footnotes Provide Acronym Explanations)

Sector/type	Emissions data source	Original spatial/temporal resolution	Spatial distribution	Temporal distribution
Onroad	EMFAC[a] CO_2, EPA NEI[b] onroad CO_2	Spatial resolution: county; Temporal resolution: annual; Categories: road class, vehicle class	FHWA AADT[c] to roadways	CCS[d] to hourly
Electricity production	CAMD[e] CO_2, DOE/EIA[f] fuel, EPA NEI point CO	Spatial resolution: Lat/lon; Temporal resolution: hourly/monthly; Categories: fuel type, technology	EPA/EIA NEI lat/lon, Google Earth (correcting coordinates)	CAMD, EIA and EPA all to hourly
Residential nonpoint buildings	EPA NEI nonpoint CO	Spatial resolution: county; Temporal resolution: annual; Categories: fuel type	FEMA HAZUS[g], DOE RECS NE-EUI[h] to US Census block-group	eQUEST[i] model to hourly
Nonroad	NEI nonpoint CO	Spatial resolution: county; Temporal resolution: annual; Categories: vehicle class	EPA spatial surrogates (vehicle class specific)	EPA temporal surrogates (by SCC[j]) to hourly
Airport	EPA NEI point CO	Spatial resolution: lat/lon; Temporal resolution: hourly/daily; Categories: aircraft class	Lat/Lon	LAWA & OPSNET[k] to houlrly
Commercial nonpoint buildings	EPA NEI nonpoint CO	Spatial resolution: county; Temporal resolution: annual; Categories: fuel	FEMA HAZUS, DOE CBECS NE-EUI[l]	eQUEST model to hourly
Commercial point sources	EPA NEI point CO	Spatial resolution: lat/lon; Temporal resolution: Categories: fuel type, combustion technology	EPA NEI Lat/Lon, Google Earth	eQUEST model to hourly
Industrial point sources	EPA NEI point CO	Spatial resolution: lat/lon; Temporal resolution: annual, Categories: fuel type, combustion technology	EPA NEI Lat/Lon, Google Earth	EPA temporal surrogates (by SCC) to hourly
Industrial nonpoint buildings	EPA NEI nonpoint CO	Spatial resolution: county; Temporal resolution: annual; Categories: fuel type	FEMA HAZUS, DOE MECS NE-EUI[m]	eQUEST model to hourly
Commercial Marine Vessels	EPA NEI nonpoint CO	Spatial resolution: county; Temporal resolution: annual; Categories: fuel type, port/underway	EPA port and shipping lane shapefiles	Flat time structure to hourly
Railroad	EPA NEI nonpoint CO, EPA NEI point CO	Spatial resolution: county; Temporal resolution: annual; Categories: fuel type, segment	EPA NEI rail shapefile and density distribution	Point records: EPA temporal surrogates (by SCC) to hourly. Nonpoint: flat time structure to hourly
Cement	Portland Cement Association, USGS	Spatial resolution: lat/lon; Temporal resolution: annual	PCA lat/lon checked in Google Earth	Flat time structure to hourly

[a]Emissions Factors Model. [b]Environmental Protection Agency, National Emissions Inventory. [c]Federal Highway Administration, Annual Average Daily Traffic. [d]Continuous Count Stations. [e]Clean Air Markets Division. [f]Department of Energy/Energy Information Administration. [g]Federal Emergency Management Agency. [h]Department of Energy Residential Energy Consumption Survey, non-electric energy use intensity. [i]Quick Energy Simulation Tool. [j]Source Classification Code. [k]Los Angeles World Airport, The Operations Network. [l]Department of Energy Commercial Energy Consumption Survey, nonelectric energy use intensity. [m]Department of Energy Manufacturing Energy Consumption Survey, nonelectric energy use intensity.

2.1.1. Nonpoint Sources

The area or nonpoint source emissions (dominated by the residential and commercial economic sectoral categories) are stationary sources that are not inventoried at the individual facility or building scale and can be thought of as representing dispersed sources within a geographic area. Vulcan nonpoint $FFCO_2$ emissions, like all the source type/sectors, are estimated using a number of individual data sources. Foremost among these are the United States Environmental Protection Agency (USEPA) National Emission Inventory (NEI) nonpoint reporting for carbon monoxide (CO) emissions, version 2 for the year 2011 (United States Environmental Protection Agency, 2005a). The NEI is a comprehensive accounting of all criteria air pollutants (CAPs) and hazardous air pollutants (HAPs) across the United States (United States Environmental Protection Agency, 2005a). The NEI now includes greenhouse gases (GHGs) for specific sectors (onroad, nonroad). The NEI is the data structure by which the USEPA meets mandates established by the Clean Air Act (CAA). The CAP emissions, the portion of emissions used by the Vulcan system (other than onroad, nonroad, and electricity production), are collected under the Air Emissions Reporting Rule (40 CFR Part 51) (Code of Federal Regulations, 2008). The NEI can be used to track progress, drive air quality modeling, facilitate emissions trading, and ensure emissions reporting and compliance.

The emissions data within the NEI are collected from state, local, and tribal (SLT) agencies further augmented by federal data sets such as the Toxics Release Inventory (TRI), the Acid Rain Program (ARP), and the Federal Highway Administration (FHWA) traffic counts.

The USEPA provides recommendations to SLT agencies on nonpoint source emissions collection guidance and the SLT agencies have a number of options in forming the basis of the reported information (Eastern Research Group, Inc., 2001). The USEPA prefers emissions to be estimated by extrapolation from a sample set of activity data to the entire population, but a number of other approaches are acceptable including material balance, mathematical models, and emission factors (EFs). This means that the method employed will vary by location. The USEPA will augment the submitted data as a result of recognized data gaps, QA/QC procedures, or in consultation with SLT agencies.

The 2011 NEIv2 nonpoint data used in the Vulcan emissions estimation is composed of two central data files. These data files share common, required key fields. The fundamental nonpoint "unit," as pertains to the Vulcan calculations, is a reported combustion process emitting carbon monoxide (CO) identified by a single source classification code (SCC) in a single U.S. county burning an identified fossil fuel. The numerical SCC (United States Environmental Protection Agency, 1995) and FIPS values (which identifies the state and county via numerical ID) are critical common IDs. Reporting associated with fugitive emissions (noncombustion), chemical or "in-process" activities, or resulting from the combustion of biogenic fuel sources are removed. An exception to this is the in-process emissions associated with cement production; however, these emissions are generated with different data outlined in a later section. Fuels considered in the Vulcan nonpoint $FFCO_2$ estimation along with their thermodynamic heat value, default CO emission factor (EF), and CO_2 EF are provided in the supporting information, Table S1.

Fossil fuel CO_2 emissions are created from NEI-reported county-scale CO reporting through the application of CO and CO_2 emission factors, as follows:

$$E_{n,f}^{CO_2} = \frac{E_{n,f}^{CO}}{EF_{n,f}^{CO}} EF_{n,f}^{CO_2} \tag{1}$$

where $E_{n,f}^{CO_2}$, are the CO_2 emissions for a process n (e.g., industrial 10 MMBTU boiler, industrial gasoline reciprocating turbine) and fuel f (e.g., natural gas, bituminous coal); $E_{n,f}^{CO}$ are the equivalent amount of CO emissions for a process n and fuel f; $EF_{n,f}^{CO}$ is the CO emission factor for a process n and fuel f; and $EF_{n,f}^{CO_2}$ is the CO_2 EF for a process n and fuel f. The CO EF is retrieved from two categories of source information: (1) "self-reported" values (supplied by state or federal air quality specialists submitting the CO emissions reporting: ftp://newftp.epa.gov/air/nei/2011/doc/2011v2_supportingdata/nonpoint/) or (2) "default" values generated from a combination of values retrieved from the USEPA WebFIRE EF database (https://cfpub.epa.gov/webfire/) and values accumulated through literature review (see supporting information Table S1 and table footnotes for details). The self-reported CO EF values are assessed for reliability and replaced by a default value if the self-reported value is less than 0.1 or greater than 5 times the identified default value.

The state total $FFCO_2$ emissions calculated as described above are compared to sector and fuel-specific fuel consumption totals reported by the Department of Energy/Energy Information Administration (DOE/EIA) State Energy Data System (Department of Energy/Energy Information Administration, 2018). The EIA SEDS consumption data are gathered to create a historical time series of energy production, consumption, prices and expenditures for members of congress, federal and state agencies, and the general public in addition to supporting EIA energy modeling analysis. The consumption in energy units are converted to $FFCO_2$ using CO_2 EFs for each fuel type category (natural gas, petroleum, coal) from values supplied in the supporting information, Table S1. Because the EIA SEDS does not separately report nonpoint versus point sources for a given sector/fuel combination, the sum of the Vulcan nonpoint and point (see next section) $FFCO_2$ emissions are compared to the EIA/SEDS totals. Adjustment of the Vulcan state/sector/fuel totals are made to the nonpoint residential and commercial sectors only, and for natural gas and petroleum fuel (aggregate) only. This is due to the understanding that the EIA SEDS survey sampling in the industrial sector is more uncertain due to the variety of fuel consumption circumstances and idiosyncratic contractual

arrangements made between utilities/fuel suppliers and industrial entities. Furthermore, industrial facilities have the capability to "stockpile" fuel, making annual consumption data difficult to interpret without the necessary stockpile information. This, and the fact that the coal-based emissions are small to nonexistent in the residential and commercial sectors, is why adjustment is not made for coal fuel values. The adjustments made to the nonpoint residential and commercial $FFCO_2$ emission amounts are shown in the supporting information, Table S2.

Subcounty distribution of the county/sector/fuel-specific $FFCO_2$ emissions to U.S. Census block groups uses the total floor area (m^2) of buildings (specific to a building class) within each U.S. Census block group combined with estimates of energy use intensity (EUI). The general approach follows

$$TE^{bg}_{n^3,f} = TFA^{bg}_{n^1} \times EUI^{cd}_{n^2,f} \left\{n^1 \rightarrow n^2 \rightarrow n^3\right\} \quad (2)$$

where the total emissions, *TE*, associated with a building of type, *n*, using fuel, *f*, in a block-group, *bg*, is equal to the product of the total floor area, *TFA*, and the energy use intensity, *EUI*, of buildings in a census division, *cd*. Because the data sources have somewhat different building type classification schemes, a crosswalk between the various categories is needed.

Building floor area is retrieved from HAZUS General Building Stock data collected and compiled by the Federal Emergency Management Agency (FEMA, 2017). Using multiple sources including the U.S. Census and the DOE, the FEMA floor area provides an estimate of the building floor area for each U.S. Census block-group specific to a classification of building types in the residential, commercial and industrial sectors. The data sources are primarily reflective of conditions in 2010 and remain unchanged over the 6 years of Vulcan output.

The nonelectric energy use intensity (NE-EUI; J/m^2) values are compiled by the DOE from building consumption energy surveys in different regions of the United States. The NE-EUI values were calculated from data in the DOE/EIA Commercial Buildings Energy Consumption Survey (CBECS, 2016), Manufacturing Energy Consumption Survey (MECS, 2010), and Residential Energy Consumption Survey (RECS, 2013) microdata which represent regional (9 U.S. Census Divisions) surveys of building energy consumption categorized by building type, fuel, and age cohort. The three data sources represent survey conditions in 2012, 2009, and 2010, respectively. A crosswalk is created linking the FEMA building types to the DOE/EIA building types (supporting information, Table S3). For the industrial sector, data are insufficient to support specificity to U.S. Census Division. Hence, the national average results are used but specific to industrial NAICS category and fuel category. Where insufficient data existed to support Census Division-specific NE-EUI values in any of the three sectors, an average was calculated using all other division/building type/fuel-specific NE-EUI values.

The product of the total building area for a given Census block-group/sector/building type combination and the sector/building type/fuel NE-EUI values act as a distributional fraction of the county total county/sector/fuel $FFCO_2$ to each U.S. Census block group. Hence this acts to provide a relative distribution of building $FFCO_2$ emission within a U.S. county only.

The time distribution of the annual $FFCO_2$ emissions for the nonpoint data source uses a building energy model, eQuest, to generate simulated building energy consumption which, in turn, is used to represent hourly time patterns (Hirsch & Associates, 2004). The eQuest simulations are based on a series of building prototypes which must be related to the FEMA building typology (in turn, related to the final Vulcan building types—see supporting information, Table S3) of the Vulcan system. This relationship is shown in the supporting information, Table S4.

To capture the local weather/climate conditions, the eQuest model is additionally driven by the 1,020 "TMY3 weather station data sets (http://doe2.com/Download/Weather/TMY3/) from the DOE (Marion & Urban, 1995). The weather statistics reflect the 1991–2005 climatological mean conditions. The resulting simulations are used to generate hourly fractional energy consumption for each of the weather station locations and for each of the building types listed in the supporting information Table S4. The closest weather station location to each of the U.S. Census block-group centroids is used to assign these hourly fractional time series to a given block-group/building type combination.

2.1.1.1. Uncertainty

Nonpoint source uncertainty is applied to the reported CO emissions, the CO EF, and the CO_2 EF. For the reported CO emissions, an uncertainty value of ±12.8% was used, a value reported by Gately and Hutyra (2017) for the residential sector (which dominates the nonpoint sources) and based on a state-scale difference between ACES and EIA state residential fuel consumption. We interpret this as a 95% confidence interval given that this is estimated from a measure of difference by Gately and Hutyra (2017). We adopt this value and apply it to each nonpoint CO emission reporting record in the 2011 NEI v2, used as county-scale input to the Vulcan nonpoint estimation.

For the EF uncertainty, the CO and CO_2 EFs were adjusted in combination such that the outcome achieves the hi and lo CI, respectively. For example, the upper/lower CI bound for the CO EF was combined with the lower/upper CI bound for the CO_2 EF to achieve the hi/lo $FFCO_2$ emissions output CI bound. An uncertainty of ±20% is applied to both the default and self-reported CO EFs regardless of fuel type. An exception to this is for the "blast furnace gas" and "coke oven gas" fuel types in which the adjustment is ±35% (Table S5). The CO EF adjustment is based on estimates of the range found in the WebFIRE database and the self-reported CO emission factors. The CO_2 EF uncertainty for coal is derived from the work of Quick (2010) while uncertainty for petroleum fuels and natural gas are derived from USEPA Greenhouse Gas Inventory, Annex 2 (United States Environmental Protection Agency, 2017). These emission factor uncertainties are applied at the county spatial-scale but specific to SCC, as described in Equation 1.

These uncertainties are propagated through all subsequent steps such as the allocation to subcounty spatial scales and subannual temporal scales. No further increase or adjustment to the uncertainty is performed in those sectors where additional downscaling, in space (from county to Census block group) or time (from annual to hourly), is made. Furthermore, the final uncertainty for a given spatial aggregation (e.g., county, state) will vary depending upon the mix of SCC-specific emissions in the aggregations.

2.1.2. Point Data

The point emissions represent facilities with a physically identifiable emission "stack" or point location and exceed a specific criteria air pollution threshold (United States Environmental Protection Agency, 2015c). The NEI point source data files are primarily composed of processes associated with the industrial and airport sectors but emissions from the commercial, railroad, nonroad, and electricity production sectors are present as well (United States Environmental Protection Agency, 2015a).

A number of key fields that define a point location for the purposes of the Vulcan $FFCO_2$ emissions estimation within the point database and include the state and county FIPS code, the "state facility identifier" (which identifies the individual emitting facility) and the tribal code (used in place of the FIPS in tribal lands). Each site or facility can have multiple emission points (different "stacks"), units (different buildings or portions of a complex facility or site), or emission processes (e.g., energy production, heaters, engines). Some of the emitting points/units/processes can have different geocoded locations and these are retained in the Vulcan processing. These were not systematically inspected for location accuracy except in urban domains associated with the Hestia Project: the Los Angeles Basin, Baltimore, Salt Lake City, and Indianapolis (e.g., Gurney et al., 2018; Gurney, Patarasuk, et al., 2019).

Each point emission record is also associated with an SCC which is used to retrieve the needed CO and CO_2 EFs to enact the same procedure outlined in the description of the nonpoint source processing. In the case of the point sources, no self-reported EFs are supplied. Separation is first made between airport point sources (processing of which is described in a later section) and nonairport point sources. The nonairport point sources are matched to a CO EF via the SCC from the USEPA's WebFIRE EF database as the first choice for the CO EF. Where no match is found, default CO EF values are used, themselves archived from literature review (see Table S1) and determined through a combination of the sector and fuel.

All point source emission records designated as industrial, railroad, and nonroad are distributed to hourly temporal resolution from the 2011 annual total using SCC-specific temporal surrogate profiles provided by the USEPAs Clearinghouse for Inventories and Emissions Factors (CHIEF) (United States Environmental Protection Agency, 2015c). The temporal surrogate profiles are constructed from monthly, weekly and diurnal cycles (data available at: ftp://newftp.epa.gov/air/emismod/2011/v3platform/ancillary_data/ge_dat_for_2011v3_temporal.zip). These temporal surrogates are composed of three cyclic time profiles (diurnal, weekly, monthly) specific to SCC that are combined to generate hourly

Table 2
Summary Information for 2011 Electricity Production Facilities in Vulcan Version 3.0

Data source	Number of facilities	Total $FFCO_2$ emissions (MtC/year)
CAMD	1,479	592.1
EIA	2,256	40.00
NEI	11,832	8.87
Total	15,567	641.0

SCC-specific time fractions for an entire calendar year. Records which do not have an SCC match are distributed as a constant hourly emission.

2.1.2.1. Uncertainty

Point source uncertainty is applied to the reported CO emissions, the CO EF, and the CO_2 EF. For the reported CO emissions, an uncertainty value of ±7.8% is used, a value reported by Gately & Hutyra, 2017) for the industrial and commercial sectors (which dominate the point sources) and based on a state-scale difference between ACES and EIA state industrial + commercial fuel consumption. We interpret this as a 95% confidence interval given that this is estimated from a measure of difference by Gately and Hutyra (2017). We adopt this uncertainty value and apply it to each point CO emission reporting record in the 2011 NEI v2 (at the stack reporting spatial scale), used as input to the Vulcan point estimation.

For the default EF uncertainty, the CO and CO_2 EFs were adjusted in combination following the same procedure described in the nonpoint source section and the same percentage numerical boundaries described there were used. For the records that use the WebFIRE CO EFs, an uncertainty value of ±20% is used for the 95% CI bounds.

These uncertainties are propagated through all subsequent steps and the final uncertainty for a given spatial aggregation (e.g., county, state) will vary depending upon the mix of SCC-specific emissions in the aggregations. Point data, being already quantified with uncertainty at the ultimate spatial resolution, requires no additional uncertainty adjustment in space. However, application of the hourly time resolution from the original annual time resolution is accompanied by no further increase or adjustment to the uncertainty.

2.1.3. Electricity Production

Three sources of data are used to estimate the $FFCO_2$ emissions at 15,566 electricity production facilities, all are geocoded to a physical location (Table 2). The first is the Environmental Protection Agency's Clean Air Markets Division (CAMD) data (United States Environmental Protection Agency, 2015b). The second is the Department of Energy's Energy Information Administration (EIA) reporting data (Department of Energy/Energy Information Administration, 2003). The third is the reporting done within the NEI point source reporting (described previously). Overlap exists between these three data sources (corrected in the processing here) which is corrected according to the prioritization in the order listed above. A detailed comparison made between the CAMD and EIA $FFCO_2$ emissions along with greater detail regarding data sources, data processing and procedures can be found in Gurney et al. (2016).

The CAMD data are collected under the Acid Rain Program (ARP), which was instituted in 1990 under Title IV of the Clean Air Act (Code of Federal Regulations, 2008; United States Environmental Protection Agency, 2005b, 2010). Though the CAMD data set does not include all power plants in the United States, it accounts for a very large proportion. The CAMD data used in Vulcan are reported as hourly CO_2 emissions monitored from an emitting stack or through a calculation, based on records of fuel consumption (ftp://ftp.epa.gov/dmdnload/emissions/hourly/monthly/). The annual reporting is also used for additional information related to the facility (http://ampd.epa.gov/ampd).

The EIA data set is derived from the EIA reporting form 923, which reports monthly data on receipts and cost of fossil fuel, fuel stocks, generation, consumption of fuel for generation, and environmental data at each power plant (http://www.eia.gov/electricity/data/eia923). Fuel consumption is reported as a heat input value (e.g., British thermal units). CO_2 emission factors are then utilized to calculate the quantity of CO_2 emitted. In order to maintain consistency with the data source, the CO_2 emission factors used by the EIA are adopted to estimate the $FFCO_2$ emissions from these facilities (Department of Energy/Energy Information Administration, 2011).

Some manual corrections are performed to the geocoordinates of both the CAMD and EIA electricity production data, as a result of searching in Google Earth or via alternative online information resources (e.g., utility websites).

A hierarchy was employed given that there was overlap between the two data sets. This was performed at the unit level given that a single facility might have individual power units reporting to CAMD and another only

reporting to the EIA. Where overlap did exist at this scale, preference was made to retain the CAMD data. Further details and rationale can be found in Gurney et al. (2016).

The CAMD reporting data is archived at the hourly temporal scale and directly used in Vulcan. The EIA electricity production reporting is resolved at the monthly scale. This is transformed into hourly reporting using a "flat" time profile or a constant level such that the monthly integral matches the reported monthly emissions data. The electricity production facilities reported in the NEI as point sources also use a flat time profile but instead of distribution over each of the reported months, the emissions are held constant over an entire year.

2.1.3.1. Uncertainty

Gurney et al. (2016) found that one fifth of U.S. power plants had monthly $FFCO_2$ emission differences exceeding −6.4%/+6.8% for the year 2009 (the closest analyzed year to the 2011 base year presented here). The emissions distribution of the two data sets were not normally distributed nor were the differences. Hence, a typical gaussian uncertainty estimate cannot be made—rather, the difference distribution was represented by quintiles of percentage difference. Hence, these values cannot be cast within the context of other normally distributed errors. However, we conservatively consider the quintile value (the positive and negative tails) as a one-sigma value and ±13% as a 95% CI boundary value. This uncertainty is applied at the facility spatial scale. Since over 90% of the $FFCO_2$ emissions in the electricity production sector are quantified at the facility/hourly space/time scale, no further adjustment to the uncertainty is made.

2.1.4. Onroad

County scale $FFCO_2$ emissions are retrieved from the 2011 USEPA NEIv1 onroad results (United States Environmental Protection Agency, 2011). The 2011 NEI onroad results report emissions for every U.S. county by 13 vehicle types (designating vehicle class and fuel) and 12 road types, including urban and rural distinctions. It is based on simulations using the Motor Vehicle Emissions Simulator (MOVES) model with inputs supplied to a county database (CDB) by SLT agencies (United States Environmental Protection Agency, 2012, 2015a). Version 1.0 of the 2011 NEI includes 1,363 CDB submissions out of a total of 3,234 counties. In order to generate results for all U.S. counties, the USEPA used multiple data and modeling tools to estimate county-specific $FFCO_2$ emissions including identifying "representative" counties among the data supplied by SLT agencies to best match those there were not reported.

The state of California did not report $FFCO_2$ to the 2011 NEI. Hence, the Vulcan onroad $FFCO_2$ emissions for California used the 2011 results from the Emissions FACtors 2014 model (EMFAC2014), produced by the California Air Resources Board (California Air Resources Board, 2014). The EMFAC2014 model estimates vehicle miles traveled (VMT) and $FFCO_2$ emissions for 27 vehicle types (reduced here to 13 via aggregation) using emissions rates ($FFCO_2$/distance traveled) and data on the California vehicle fleet and activity statistics such as VMT, speed distributions, and idle times (California Air Resources Board, 2015). Distribution to sub-state scales uses annual vehicle counts from the Highway Performance Monitoring System (HPMS). The HPMS is a spatial road network database managed by the FHWA to monitor and record Average Annual Daily Traffic (AADT) counts (Federal Highway Administration, 2014). By considering vehicle registration in combination with the HPMS data, EMFAC also accounts for interregional travel.

County-scale $FFCO_2$ emissions for all U.S. states are spatially assigned to road segments using a road basemap representing the entire road surface potentially occupied by onroad vehicles. Vulcan uses a combination of the 2011 Highway Performance Monitoring System (Highway Performance Monitoring System, 2017) road network and Open Street Map (OSM; http://download.geofabrik.de/) road network. The Census Urbanized Areas boundary (https://www.fhwa.dot.gov/policyinformation/hpms/shapefiles.cfm) was used to assign an urban/rural classification to each of the seven original HPMS road classes making them compatible with the NEI road classes (Table S6).

The distribution of county-scale road/vehicle-specific $FFCO_2$ emissions along the complete length of road class in a county, is achieved through the use of the 2011 AADT data from the FHWA's HPMS (http://www.fhwa.dot.gov/policyinformation/hpms/shapefiles.cfm; state scale data files were used). AADT counts are collected using short-term and continuous counting methods. Most data are collected by individual states and reported to the FHWA, but some data are also collected by the FHWA directly. Very little AADT data was collected on local roads (urban local, rural local). For those segments in our merged basemap that do not have an AADT value, gap-filling techniques were used (see Text S2 for details on gap-filling methods).

With a complete U.S. map of AADT values and road segment length, the vehicle miles traveled (VMT) can be estimated. The fraction of a non-local road class-specific road segment's VMT within a county acts as the distribution means to allocate county-scale onroad $FFCO_2$. For local roads, given the paucity of AADT data, the fraction of a road segment's length out of all local roads within a county acts as the allocation method. Hence, the local roads have no emission gradients along the local roads (at the subcounty scale). There are general $FFCO_2$ emissions gradients in space, however, dictated by the spatial density of local roads.

In order to use the spatial distribution methods employed by the Vulcan system and be compatible with the NEI results for the other U.S. states, vehicle class/county-specific California onroad $FFCO_2$ emissions were translated to the six vehicle classes and 14 road classes (seven of urban and rural subtypes) in the NEI. This was performed using the FHWA state-scale road class-specific VMT data and the proportion of VMT by vehicle class. Details are provided in the supporting information, Text S2.

After completing the spatialization procedure across all counties in the United States, it became clear that there were some mismatches between NEI road class VMT and the AADT on the HPMS road network. For example, there were instances in which onroad $FFCO_2$ emissions were present in a county for a particular road class, but for which no AADT data existed and vice-versa. These mismatches could be due to the demarcation of urban versus rural roads. As noted previously the roads were divided into urban and rural classes based on the U.S. Census Urbanized Areas. This may differ from the choices made when state officials were generating the county database inputs for the USEPA (e.g., if the NEI estimate uses state-supplied data in the MOVES onroad emissions estimate). While the HPMS AADT data has an urban code, we used the U.S. Census Urbanized Areas to divide a road classes so that the urban/rural classification would be consistent between the OSM and HPMS basemaps.

In cases where emissions were reported for a road class in the NEI, but for which there were no physical roads in our AADT gap-filled road basemap, the emissions reported in NEI were moved to the next closest road class containing AADT data. The closest road class is the urban or rural counterpart within the same class-size, and the second-closest being the road class that is the next class-size down. In cases where AADT was present for a road class, but no NEI $FFCO_2$ emissions were reported for that road class, $FFCO_2$ emissions were redistributed from the next closest road class, proportional to VMT. For example, if the NEI reports emissions for urban interstates, but VMT was estimated for both urban and rural interstates, then the NEI reported emissions would be redistributed from urban interstates to rural interstates proportional to the VMT in each road class.

In the state of California, the EMFAC results were crosswalked from county-scale, vehicle class-specific $FFCO_2$ emissions to totals that include road class. These $FFCO_2$ emissions were distributed onto road segments in the same manner as done for other states. However, unlike other states, there were no cases in which the EMFAC onroad $FFCO_2$ emissions needed to be "shuffled" to partner road classes.

Hourly traffic volume data for 2011–2013 were obtained from the FHWA Continuous Count Stations (CCS) data set (previously known as the Automatic Traffic Recorder; ATR) (https://www.fhwa.dot.gov/policyinformation/tables/trafficmonitoring/). The CCS stations measure hourly traffic volume at a fixed location in space and we use that latitude and longitude as a unique station identifier. Additional corrections were made to the Connecticut station coordinates based on data from the Connecticut Department of Transportation (http://www.ct.gov/dot/cwp/view.asp?a=1383&q=330402).

For each station, the direction(s) and lane(s) of traffic are aggregated to estimate the total hourly traffic volume moving through a station across all lanes and directions. Any station for which missing data exceeded six months (either contiguous or not) were removed from the data set. This left a total of 5,106 traffic volume monitoring stations in the year 2011, 5,172 in 2012, and 5,527 in 2013. The year 2011 contained 141 stations that were not present in either 2012 or 2013. The year 2012 contained 57 stations that were not present in either 2011 or 2013 and 2013 contained 511 stations that were not present in either 2011 or 2012. Each year of the traffic monitoring data (for which data gaps did not exceed 6 months) are gap-filled individually, maintaining the cyclic integrity of hour-of-day and day-of-week. Details are provided in Text S2.

After combining the 2011, 2012, and 2013 CCS data into a single average year data set, there were a total of 5,890 stations in the Continental United States, and these are used for the construction of the temporal profiles.

In order to distribute the temporal distribution measured at the gap-filled CCS measurement stations to all road segments in the United States, interpolation/extrapolation of the traffic patterns is required. Given the paucity of traffic measurement stations relative to the total area of the U.S. landscape and the fact that the temporal distribution of traffic is less related to road class than space, the eight road original classes in the temporal data were aggregated/combined to four for purposes of spatial interpolation of the time structure. There is evidence that interstates have unique traffic patterns from all other road classes due to the dominance of commercial interstate trucking. Furthermore, interstate traffic in cities is a mix of passenger vehicles and commercial trucking while rural interstates are dominated by commercial trucking. Hence, the road classes chosen for the purposes of temporal interpolation were: rural interstate, urban interstate, rural non-interstate, and urban non-interstate. Figure S3 in the supporting information shows the CCS measurement locations aggregated to these four temporal road classes.

Inverse Distance Weighted (IDW) interpolation was performed for each of the four temporal road classes separately and only for grid cells containing that road class. The IDW used the default number of neighbors (all neighbors), and the default power function (2), making this an inverse distance squared method.

2.1.4.1. Uncertainty

The uncertainty in the onroad sector uses the results from Gately and Hutyra (2017) which, in turn, references Gately et al. (2013) and Mendoza et al. (2013). This uncertainty was estimated at ±7.1% for a presumed 1-sigma uncertainty at the 1 km^2/annual resolution. Here, we have assigned ±14.2% to the 95% CI boundaries for all road types. These uncertainties are applied at the county/annual space/time scale and are propagated through all subsequent steps such as the allocation to sub-county road segments and subannual temporal scales. No increase in the uncertainty is made during the allocation steps.

2.1.5. Nonroad

The nonroad sector $FFCO_2$ emissions estimates are retrieved from the 2011 USEPA NEIv2 which uses the NONROAD model to estimate emissions (ftp://ftp.epa.gov/EmisInventory/2011/2011neiv2_nonroad_byregions.zip) across a large number of mobile sources that travel "off-road" (United States Environmental Protection Agency, 2015a) except locomotives, airplanes and commercial marine vessels (CMV) which are taken up in separate sections in this document. The NONROAD model results, in turn, are based on output from the National Mobile Inventory Model (NMIM) which relies on data inputs from the National County Data base (NCD) (United States Environmental Protection Agency, 2005c, 2005d). Both the NMIM and the NCD were described previously (Gurney et al., 2009). The USEPA updated data within the NCD from 12 SLT agencies along with USEPA default values to generate the results in the 2011 NEIv2 (for a description of these updates see ftp://ftp.epa.give/EmisInventory/2011/doc/2011neiv2_supdata_nonroad).

As with the onroad sector, California presents a special case. The CO emissions are reported comprehensively using California's OFFROAD model (www.arb.ca.gov/msei/offroad/offroad.htm) but no CO_2 was reported. Hence, California CO emissions have been scaled by the mean SCC-specific CO_2/CO ratio from all other U.S. counties.

Spatial distribution uses the spatial surrogates generated by the USEPA reflecting a series of spatial representations such as the mines, golf course and agricultural land (shapefiles can be found here: ftp://ftp.epa.gov/EmisInventory/emiss_shp2003/us/or ftp://ftp.epa.gov/EmisInventory/2011v6/v1platform/spatial_surrogates/shapefiles/). There were instances in which nonroad $FFCO_2$ emissions could not be associated with a spatial entity due to missing data. These emissions are spatialized by first aggregating all the unassociated subcounty emission elements to the county scale for a given spatial shape (e.g., golf courses, mines) and then distributing these emissions evenly across the county.

The distribution to agricultural land is aimed at representing the $FFCO_2$ emissions associated with mobile agricultural machinery such as tractors and harvesters. The only other representations of $FFCO_2$ emissions within what is often categorized as the agricultural sector will be represented in Vulcan through commercial buildings such as greenhouses burning fossil fuel for on-site processes and point sources such as in-field heaters or smudge pots.

The subannual temporal distribution of the nonroad $FFCO_2$ emissions uses SCC-specific temporal surrogate profiles provided by the USEPAs Clearinghouse for Inventories and Emissions Factors (CHIEF) (United States Environmental Protection Agency, 2015c). The temporal surrogate profiles are constructed from

monthly, weekly and diurnal cycles (data available at: ftp://newftp.epa.gov/air/emismod/2011/v3platform/ancillary_data/ge_dat_for_2011v3_temporal.zip).

These temporal surrogates are comprised of three cyclic time profiles (diurnal, weekly, monthly) specific to SCC that are combined to generate hourly SCC-specific time fractions for an entire calendar year. There are five SCC codes present in the NEI 2011 nonroad data file but not found in the temporal surrogate files (2,260,006,035, 2,265,006,035, 2,267,006,035, 2,270,006,035, 2,268,006,035)—these were given a "flat" or constant time profile in the absence of any specified temporal distribution.

2.1.5.1. Uncertainty

Nonroad records other than those derived from the point source data files (which follow the point source uncertainty estimation described in the point source section) are assigned a 95% CI boundary of ±3.8% for the $FFCO_2$ emission value. This was derived from examination of the range of carbon content and fuel density uncertainties as outlined in United States Environmental Protection Agency (2017), Annex 2, page A-86. This is consistent with the point source uncertainty for nonroad distillate fuel consumption. These uncertainties are applied at the county/annual space/time scale and are propagated through all subsequent steps such as the allocation to subcounty spatial entities and sub-annual temporal scales. No increase in the uncertainty is made during the allocation steps.

2.1.6. Airport

As described in the point source section, the airport $FFCO_2$ emissions are estimated from the 2011 NEI point source reporting for CO. The emission factors used (Table S10) convert the reported CO emissions to $FFCO_2$ and are specific to aircraft class and fuel, consistent with the reporting in the NEI which often listed multiple processes (aircraft class/fuel) for a single airport facility. The fuel type implied by the CO_2 EF values uses jet fuel except where explicitly indicated in the SCC description (NG, LPG, diesel, gasoline).

The airport $FFCO_2$ emissions are only associated with the taxi and takeoff/landing sequences. $FFCO_2$ emissions associated with nonaircraft processes such as building operations and nonaircraft mobile sources are reported as emissions in other sectors (e.g., commercial, nonroad). The airports are geocoded to the airport location in the NEI though some manual adjustments have been made to the original coordinates using manual inspection in Google Earth. The emission point, in these instances, is placed in the middle of the central runway.

Temporal distribution of the $FFCO_2$ airport emissions use a series of data sets. The Los Angeles World Airports (LAWA) data set reports hourly flight volume for three airports in the LA Basin domain: Los Angeles International airport (LAX), Ontario airport (ONT), and Van Nuys airport (VNY). The Operations Network (OPSNET) data set from the FAA reports total date-specific, daily flight volume (365 values) at specific airports (https://aspm.faa.gov/opsnet/sys/Default.asp). An hourly time profile was constructed by combining the LAWA diurnal profile and the OPSNET annual profile. The three LAWA airports constituted the diurnal cycle (Figure S4) at all U.S. airports with the LAX assigned to international airports, the ONT to noninternational airports and the VNY to local airports.

Airports were matched with a Federal Aviation Administration (FAA) international airport database (FAAINTL) by airport code to determine whether an airport is international (https://hub.arcgis.com/datasets/4782d6f5aa844591a16d46df635b7af4_1). Airports which could not be matched to the OPSNET data by airport code/airport name were assigned a temporal invariant ("flat") hourly time structure.

FAAINTL, OPSNET, and two additional airport databases (the National Airport Atlas (NAA; https://catalog.data.gov/dataset/airports-of-the-united-states-direct-download) and AIRNAV; www.airnav.com) were used to determine whether an airport was an airport or a helipad. The name/code of each airport was searched in these airport databases. An airport which could not be identified in any of the aforementioned airport databases would be categorized as a helipad. A temporally invariant time structure was applied to all helipads.

A portion of the Vulcan v3.0 CMV $FFCO_2$ emissions would be considered "bunker" fuel combustion (i.e., consumed as part of international travel) under the IPCC reporting methodology within the UNFCCC process. Vulcan does not separate bunker from nonbunker fuel consumption and a portion of the airport sector emissions (particularly international air flights) would be considered as such were the IPCC reporting categorization applied here. No attempt has been made to limit or separately report airport emissions that would be considered part of the bunker fuel definition.

2.1.6.1. Uncertainty

The uncertainty in the airport sector is derived from the point source processing as described previously (magnitude and EF-based uncertainty) except that the $FFCO_2$ EFs are specific to the mix of aviation fuels associated with the emission records and are based on uncertainty estimation from the USEPA (2017), Annex 2, pages 85 and 89. These uncertainties are propagated through all subsequent steps and the final uncertainty for a given spatial aggregation (e.g., airport, county, state) will vary depending upon the mix of airplane classes and fuels in the aggregations. Point data, being already quantified with uncertainty at the ultimate spatial resolution, requires no additional uncertainty adjustment in space. However, application of the hourly time resolution from the original annual time resolution is accompanied by no further increase or adjustment to the uncertainty.

2.1.7. Railroad

The $FFCO_2$ emissions associated with railway activity are derived from the 2011 NEIv2 CO emissions reporting which, in turn, were developed for the 2008 NEI (Eastern Research Group, 2011) and scaled to 2011 values (Eastern Research Group, 2012). Emissions related to the railroad sector were reported as a mixture of nonpoint and point emissions and hence, these were managed separately but combined when represented as spatial entities. The CO emissions were converted to $FFCO_2$ following the procedures outlined in the nonpoint and the point sections, respectively.

The two NEI source categories imply different spatial representations, however. The point source railroad emissions are associated with rail yards and related geospecific locales and are placed in space according to the provided latitude and longitude. The railroad $FFCO_2$ emissions associated with the nonpoint NEI reporting contain an ID variable that links to a spatial element (rail line segment) in the USEPA railroad GIS shapefile (https://www.epa.gov/sites/production/files/2015-06/railway_20140730.zip). A large number of railroad emission records have no railroad segment match and are spatialized using freight statistics described in Text S2.

The annual railroad $FFCO_2$ emissions are distributed to the hourly time scale with no additional temporal structure (a "flat" time distribution), unless they originated from point source data for which the SCC-specific time profiles, previously described, are used.

2.1.7.1. Uncertainty

The uncertainty for the railroad emissions is directly inherited from the uncertainty estimation described for the point and nonpoint source processing, respectively. The only difference is related to the CO magnitude uncertainty ($\pm$3.8%) which was derived from examination of the range of carbon content and fuel density uncertainties outlined in USEPA (2017), Annex 2, page A-86 for distillate fuels, the dominant fuel used in railroad. As per the description of uncertainty application in the point and nonpoint processing, these uncertainties are applied at scale from an individual point location to the county spatial scale. The uncertainties are propagated through all subsequent steps such as the allocation to the railroad polyline map and sub-annual temporal scales. Additional uncertainty associated with downscaling in space (i.e., from county to polylines) or time (from annual to hourly) are not included in the final uncertainty estimate.

2.1.8. Commercial Marine Vessels

The $FFCO_2$ emissions associated with commercial marine vessels (CMV) rely on nonpoint NEIv2 CO emissions reporting and follow the same emission factor-related conversion outlined in the nonpoint source section. CMV includes vessels directly or indirectly involved in commerce or military activity. The emissions encompass maneuvering, hoteling, cruise and reduced speed zone travel and are specific to geographically located ports and shipping lanes that extend 12 nautical miles from the U.S. shoreline. Private or "pleasure" craft are not included as part of the CMV emissions but are captured in the nonroad reporting. As with the nonroad reporting, the USEPA used a mixture of SLT data submissions and default values, in collaboration with the Office of Transportation and Air Quality to generate an estimate of CO emissions for CMV. A portion of the Vulcan v3.0 CMV $FFCO_2$ emissions would be considered "bunker" fuel combustion (i.e., consumed as part of international trade) under the IPCC reporting methodology within the UNFCCC process. Vulcan does not separate bunker from non-bunker fuel consumption and a portion of the CMV sector emissions (particularly ship travel directed toward international waters) would be considered as such were the IPCC reporting categorization applied here. No attempt has been made to limit or separately report CMV emissions that would be considered part of the bunker fuel definition.

The spatialization utilized the USEPA shapefiles that delineate U.S. ports and U.S. shipping lanes through spatial IDs associated with the emission records (https://www.epa.gov/sites/production/files/2015-06/ports_20140729.zip; https://www.epa.gov/sites/production/files/2015-06/shippinglanes_072914.zip). In the instance that no spatial entity is identified for an emission record, a simple spatial alternative is employed whereby all the unlinked port (or "underway") emissions are summed within a county and evenly distributed to the shapes that are identified within that county (either ports or shipping lanes).

The CMV sector has no data allowing for the designation of hourly time structure. Hence, the emissions are temporally invariant over all hours of the year ("flat" distribution).

2.1.8.1. Uncertainty

The uncertainty of the CMV emissions is directly inherited from the uncertainty estimation described for the point and nonpoint source processing, respectively. The only difference is related to the CO magnitude uncertainty (±10.0%) which was derived from examination of the range of carbon content and fuel density uncertainties outlined in USEPA (2017), Annex 2, page A-87 for residual fuels, the dominant fuel used in CMV. As per the description of uncertainty application in the point and nonpoint processing, these uncertainties are applied at scale from an individual point location to the county spatial scale. The uncertainties are propagated through all subsequent steps such as the allocation to the shipping lane map and sub-annual temporal scales. Additional uncertainty associated with downscaling in space (i.e., from county to ports and ship tracks) or time (from annual to hourly) are not included in the final uncertainty estimate.

2.1.9. Cement

CO_2 is emitted from cement manufacturing as a result of fuel combustion and as process-derived emissions (Andrew, 2018). The emissions from fuel combustion are captured in the point source reporting. The process-derived CO_2 emissions result from the chemical process that converts limestone to calcium oxide and CO_2. This occurs during "clinker" production (clinker is the raw material for cement which is produced by grinding the clinker material).

Estimation of CO_2 emissions from clinker production utilizes two data sets. The first is the data provided by the Portland Cement Association which provides the annual clinker capacity at individual facilities, postal addresses, facility name, zip code and contact phone numbers (Portland Cement Company, Economic Research Department, 2006). The capacity data reflects conditions for the calendar year 2006. The other data set utilized is the Minerals Yearbook produced by the United States Geological Survey which provides the capacity factor (or percent utilization of capacity) on a statewide or multi-state basis (some states are quantified individually; others are part of an aggregate) (United States Geological Survey, 2013). The product of capacity and the capacity factor provides an estimate of clinker production.

Clinker production for 2011 is scaled from the Vulcan version 2.0 (CY 2002) estimate (Gurney et al., 2009) using the relative annual capacity factor. The CO_2 emission factor used in the Vulcan Project is 0.59 metric tons CO_2/short ton of clinker produced (Intergovernmental Panel on Climate Change, 2006).

The geolocation for each of the individual facilities was achieved by entering the PCA document's facility address into Google Earth and visually inspecting the scene for the primary emitting stack of the cement facility. This approach succeeded in locating all 105 facilities present in the PCA document.

The USEPA estimates cement manufacturing in 2011 to account for 32.2 $MtCO_2$/year (United States Environmental Protection Agency, 2017). These estimates, in turn, are based upon throughput estimates from the U.S. Geological Survey. Vulcan estimates a total of 34.6 $MtCO_2$/year which compares well with the cement manufacturing estimate from the USEPA.

The cement sector has no data allowing for the designation of hourly time structure. Hence, the emissions are evenly distributed over all hours of the year (a "flat" distribution).

2.1.9.1. Uncertainty

The uncertainty in the cement emissions sector is currently prescribed as ±10% for the 95% CI. We use a comparison between the facility-scale sum of clinker production in a state and the United States Geological Survey (USGS) state throughput (estimated from the capacity factor and capacity). The mean percentage difference across all states and multistate aggregates was 9.8%, which was rounded to 10% and interpreted as a 95% CI value. This is applied at the individual facility spatial scale and propagated through the estimation procedure. Hence, this uncertainty will remain at this value for aggregated spatial scales within this sector.

Table 3
Annual Sector Specific $FFCO_2$ (and Cement) Emission Totals for the United States, 2010–2015, Estimated by Vulcan v3.0. (Units: MtC/year)

Sector\year	2010	2011	2012	2013	2014	2015
Residential	92.0	89.2	78.5	91.3	95.3	88.0
Commercial	63.0	62.9	57.1	63.4	66.8	68.5
Industrial	230.6	228.4	227.2	233.8	237.4	231.4
Elec Prod	667.3	641.0	604.3	609.0	609.2	574.4
Onroad	452.1	440.6	436.6	443.2	448.7	452.4
Nonroad	64.2	63.3	62.4	63.5	64.6	65.2
Airport	19.8	19.6	20.5	22.3	22.3	21.8
Rail	11.9	12.0	12.6	13.7	15.1	14.6
CMV	28.4	23.3	20.9	18.5	16.2	18.1
Cement	9.6	9.70	9.80	9.80	9.80	9.80
Total	1638.9 (1,408, 1,911)	1589.9 (1,367, 1,853)	1530.0 (1,314, 1,786)	1568.5 (1,349, 1,829)	1585.2 (1,364, 1,847)	1544.3 (1,328, 1,801)

Given that cement emissions are characterized as point data no additional uncertainty adjustment is required for spatial error. However, though justified, no further increase or adjustment to the uncertainty is made for the downscaling from annual to hourly estimates.

2.2. Multiyear Estimation

The multiyear (2010–2015) results were achieved using scale factors constructed from the EIA State Energy Data System (SEDS) database (http://www.eia.gov/state/seds/). Ratios were constructed relative to the year 2011 in all SEDS sector/fuel designations for each U.S. state. This means that the spatial patterns at the sub-state scale are fixed throughout the 2010–2015 timespan for a state/sector/fuel combination. In other words, if the mixture of sector shares and fuel shares within a state varies, the spatial pattern at the sub-state scale will as well. The crosswalk from the EIA SEDS codes to a sector/fuel designation is provided in Table S11.

Exceptions to the use of the EIA SEDS database were made for the electricity production, railroad and CMV multiyear scaling. Electricity production $FFCO_2$ emissions are monitored on an hourly basis for all the output derived from the CAMD data (92.4% of the total electricity production emissions) and on a monthly basis for all of the EIA reported data (6.2% of the total electricity production emissions). The remaining NEI reported electricity production emissions (1.4% of the total electricity production emissions) use the EIA SEDS multiyear ratios.

In the case of the railroad sector, state-scale EIA specific to distillate fuel oil sales to the railroad sector was used (http://www.eia.gov/dnav/pet/pet_cons_821dsta_a_epd0_val_mgal_a.htm) to construct the year-to-year ratios relative to 2011. This data is used in generating the results in the EIA SEDS database but is aggregated and thus not as specific to the railroad sector as needed. Large year-over-year ratio values were found for a few individual years in low-population states (Nevada, Rhode Island, New Mexico, Hawaii). Values that exceeded 5.0 were replaced by the year-specific U.S. average ratio.

The procedure for the CMV $FFCO_2$ emissions is similar but combines the EIA data on distillate fuel oil sales for "vessel bunkering use" (http://www.eia.gov/dnav/pet/pet_cons_821dsta_a_epd0_vab_mgal_a.htm) with residual fuel oil sales for transportation (http://www.eia.gov/dnav/pet/pet_cons_821rsda_a_eppr_vat_mgal_a.htm). As with the railroad sector application, large year-over-year ratios were filtered (those exceeding 5.0 were replaced by the U.S. national average).

The ratio values are applied to the annual totals in each of the sector/fuel categories specific to the state FIPS code to generate a multiyear time series.

3. Results

Annual sector totals are provided in Table 3 for the 2010–2015 time period. Across all sectors, 2012 is the year with the least emissions (1,530.0 MtC/year; 95% CI: 1,314–1,786 MtC/year or −14.1%/+16.7%). While 2010

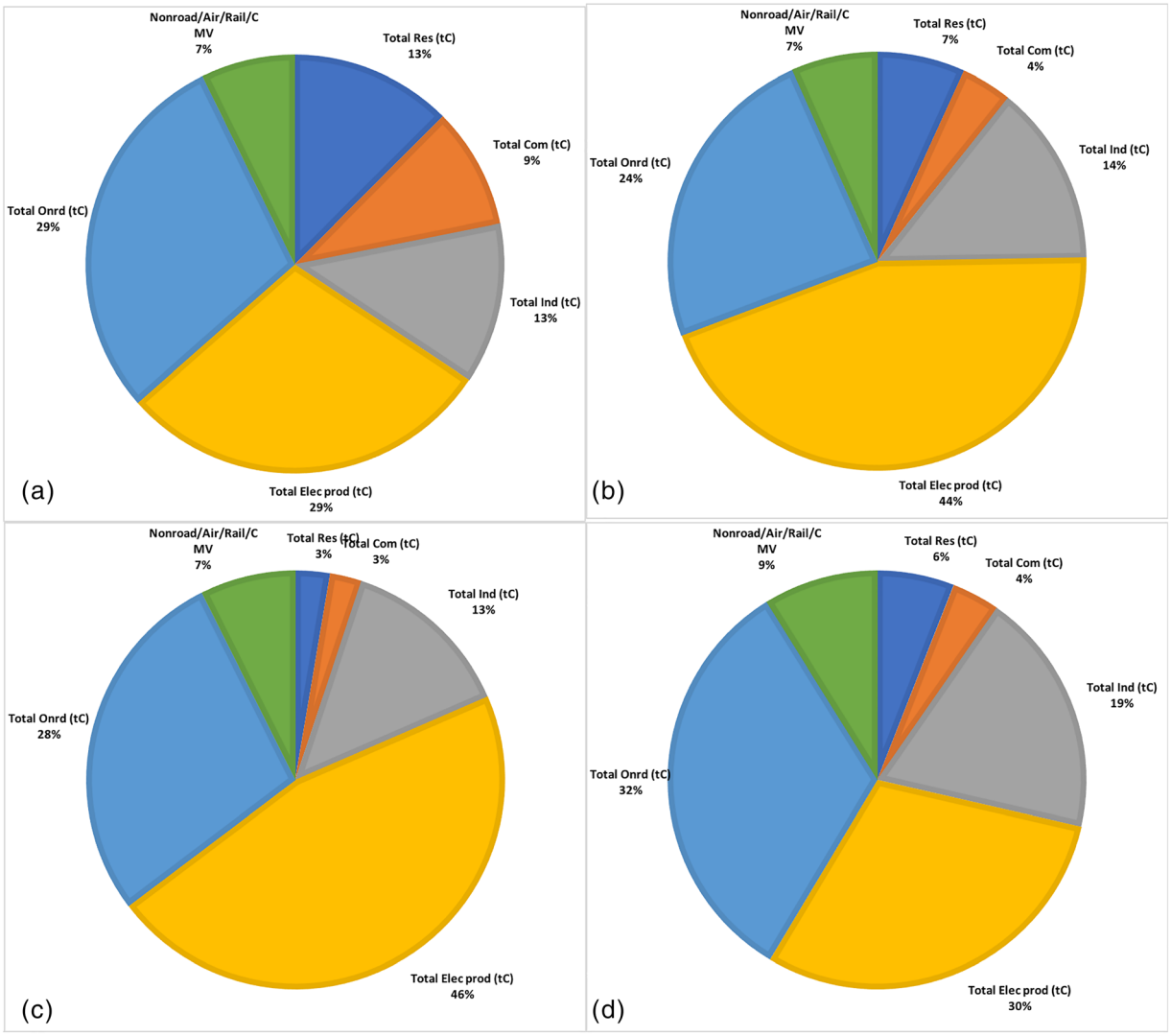

Figure 1. Sector-specific percentage share of 2011 Vulcan v3.0 $FFCO_2$ emissions for the United States by U.S. Census region: (a) northeast; (b) midwest; (c) south; (d) west.

was the largest year for total emissions (1,638.9; 95% CI: 1,408–1,911 MtC/year or −14.1%/+16.6%), the maximum value was primarily due to large $FFCO_2$ emissions in the electricity production sector. The total $FFCO_2$ emissions (plus cement) in 2015, the most recent year in the time series, were 1,543.7 MtC/year (95% CI: 1,268–1,857 or −17.9%/+20.3%), a decline driven almost entirely by electricity production $FFCO_2$ emissions. Electricity production is the largest emitting sector in all years, followed by the onroad and industrial sectors, respectively.

The order of the 2011 $FFCO_2$ emitting sectors (Figure 1) varies regionally (U.S. Census Regions) with the electricity production sector accounting for the largest share in the Midwest (44%) and South (46%) while onroad emissions account for the largest share in the West (32%) and Northeast (29%). The sum of the commercial and residential sectors is a larger share of total emissions in the Northeast (22%) than in the other three regions (6–11%). The industrial $FFCO_2$ emissions account for the largest industrial share in the West (19%) compared to the other three regions (13–14%). Overall, 2011 $FFCO_2$ emissions are largest in the South (652 TgC), followed by the Midwest (434 TgC), the West (293 TgC) and the Northeast (200 TgC).

When examined at the state-scale, the apportioning of the $FFCO_2$ emitting sectors shows a relationship to total $FFCO_2$ per capita emissions (Figure 2). States with larger per capita emissions tend to be dominated

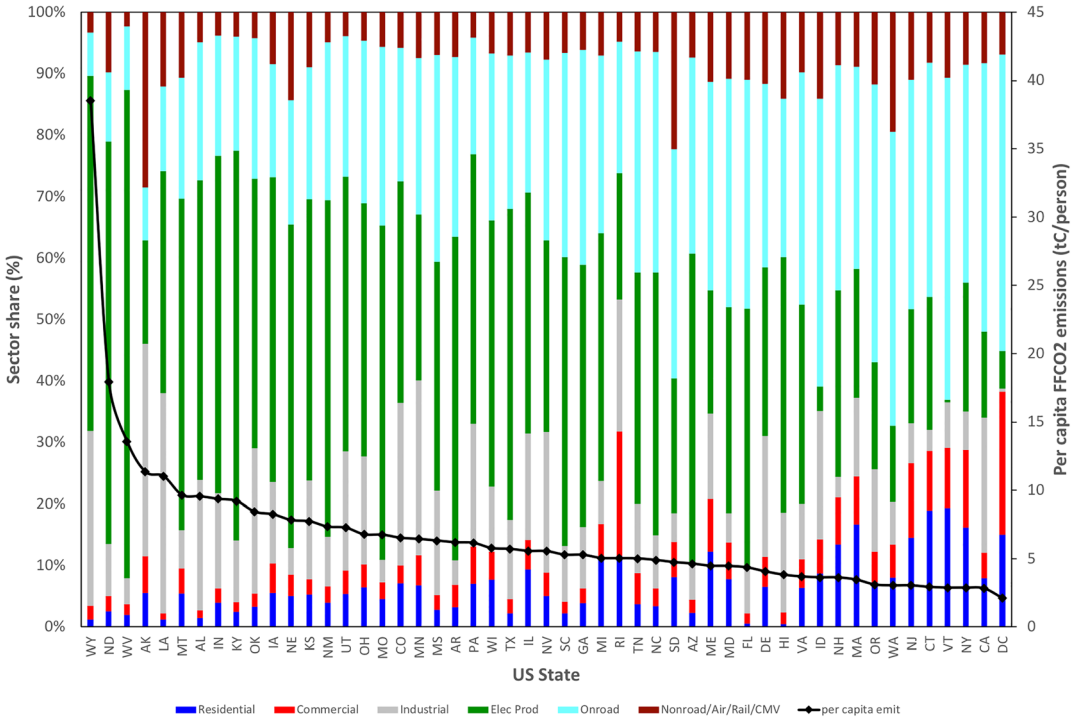

Figure 2. Vulcan v3.0 $FFCO_2$ emissions sector share (left *y* axis: %) by state and per capita $FFCO_2$ emissions (right *y* axis: tC/person) for year 2011.

by industrial and electricity production sector $FFCO_2$ emissions. States with lower per capita total $FFCO_2$ emissions tend to have lesser industrial and electricity production $FFCO_2$ emissions and a greater share of onroad and residential/commercial emissions. A few states are notable exceptions to this pattern. For example, the states of Alaska, Washington, and South Dakota have a relatively large portion of nonroad emissions while Rhode Island and Washington DC have a relatively large proportion of commercial sector $FFCO_2$ emissions. Tabular results at the state-scale are provided in Supplementary Information, Table S12.

Per capita emissions vary across the states, with the largest in the state of Wyoming (38.5 tC/person) and the smallest in Washington DC (2.11 tC/person) and California (2.81 tC/person). The median total per capita $FFCO_2$ emissions at the county-scale are 3.80 tC/person (see Figure S3 in the supporting information). It is worth noting that the population statistics used here define the population as that residing within the state which will influence the results for Washington DC where there is a large daytime non-resident population.

The Vulcan $FFCO_2$ emissions are quantified at the subnational scale according to three general shape types: points (e.g., electricity production, industrial point reporting), lines (e.g., onroad) and polygons (e.g., non-road, residential). For use in atmospheric transport modeling and ease of use in analysis, these results are gridded using a 1 km × 1 km regular grid (Figure 3a). The importance of urban areas is clearly demonstrated in the complete U.S. mapped landscape along with the greater urbanization in the eastern half of the country and along the West coast. Interstates and other large primary roadways are also evident across the U.S. connecting large population centers. Normalization by population (LandScan Geographic Information Science & Technology, Oak Ridge National Laboratory, https://landscan.ornl.gov/) offers a dramatically different perspective on U.S. $FFCO_2$ emissions, placing greater emphasis on the western half of the country (Figure 3b).

A center of mass (CoM) is a useful and compact metric to understand and illustrate the spatial changes in fossil fuel CO_2 emissions over time (Gregg et al., 2009). The CoM summarizes the distribution of emissions in the same way as the mean summarizes a probability distribution (Asefi-Najafabady et al., 2014). Figure 4 shows both the multiyear and monthly mean CoM. The multiyear CoM shows a general shift from the East to the West over the 6 years examined here with the CoM located in Missouri ~70 miles SW of St Louis, MO. The monthly mean results show a tendency to move along a NE/SW axis with wintertime movement toward

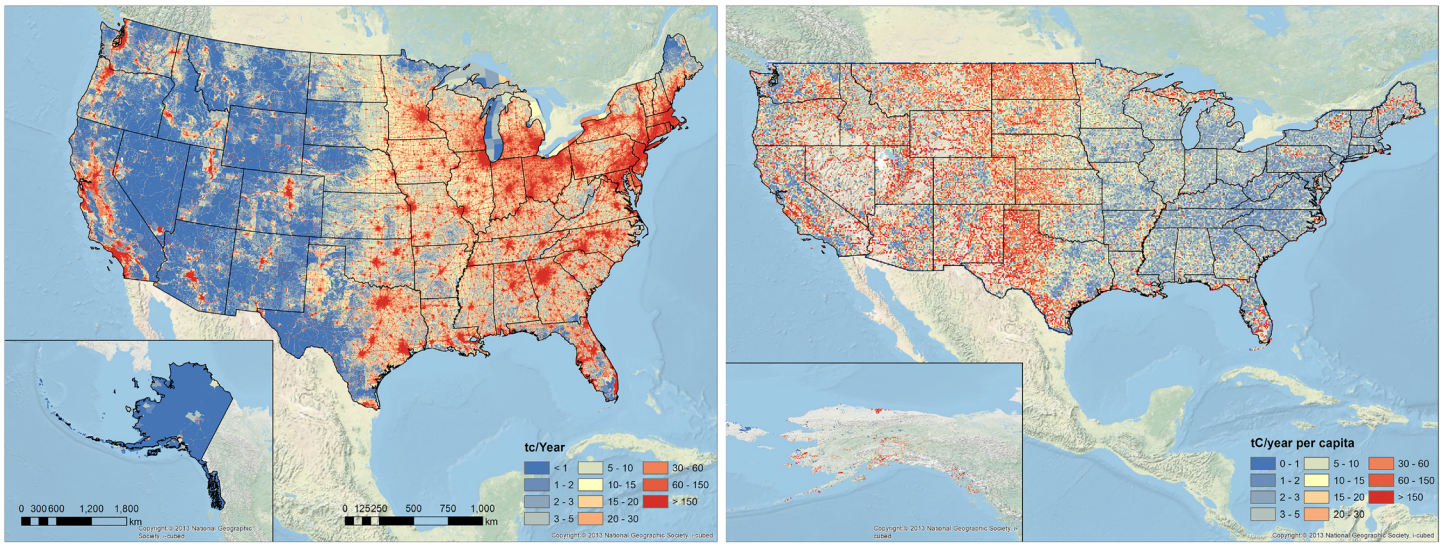

(a) (b)

Figure 3. Vulcan v3.0 2011 $FFCO_2$ emissions for the United States. (a) Absolute emissions (1 km × 1 km resolution, tC); (b) per capita emissions (0.1° × 0.1° resolution, tC; different resolution and projection required for integration with population data).

the NE driven by greater heating needs associated with cold/continental conditions. Summertime movement is toward the SW associated with the rising air-conditioning demand during summer months. The months of May/June/July show movement toward the SE in May and June, a shift toward the North in July, before resuming the Western shift in August and September.

The 2011 monthly $FFCO_2$ emissions magnitude exhibits two maxima of roughly equal value over the course of the year: a winter maximum in the months of December and January and a summer maximum in the months of July and August (Figure 5) The maxima correspond to the northernmost CoM position in the winter and near-southernmost CoM position in summer which are associated with the demand for heating in the winter, dominated by more northerly locations, and the demand for cooling in the summer, dominated by more southerly locations.

4. Discussion

The Vulcan approach to quantification of bottom-up granular $FFCO_2$ emissions established a method that has been since followed by other investigators with useful and instructive variations (e.g., Bun et al., 2018; Gately & Hutyra, 2017). Some of the differences are driven by differing national circumstances related to data availability and collection sources. A recent study estimating national $FFCO_2$ from atmospheric observations, included an aggregate comparison not just to the Vulcan v3.0 results (aggregated from 0.1° × 0.1° and monthly space/time resolution) but to three other estimates aggregated into the U.S. domain: the CDIAC, EDGAR (v4.2 and v4.3) and the USEPA (Basu et al., 2020). In that comparison for the year 2010, Vulcan v3.0 and the atmospheric-derived estimate agreed to within 1.4% but departed significantly from the other three aggregated totals, most notably the estimate by the USEPA. Though the uncertainty bounds overlapped, the USEPA central estimate was 6% lower than the total Vulcan v3.0 $FFCO_2$ emissions. A more thorough investigation into the differences between the USEPA and Vulcan estimates is warranted given the importance of the USEPA estimate to the official reporting of the U.S. to the United Nations Framework Convention on Climate Change (UNFCCC). This is an effort planned for future work.

Other than the ACES data product, which covers only the Northeast U.S. domain, there is no other U.S.-based granular estimate of $FFCO_2$ emissions with which to evaluate the results presented here. As noted in section 1, however, numerous global gridded estimates of $FFCO_2$ emissions have been constructed starting in the 1990s. Currently, only the ODIAC estimate is quantified at a resolution similar to the Vulcan data product reported here (Oda et al., 2018; Oda & Maksyutov, 2011). Hence, we perform comparison to the

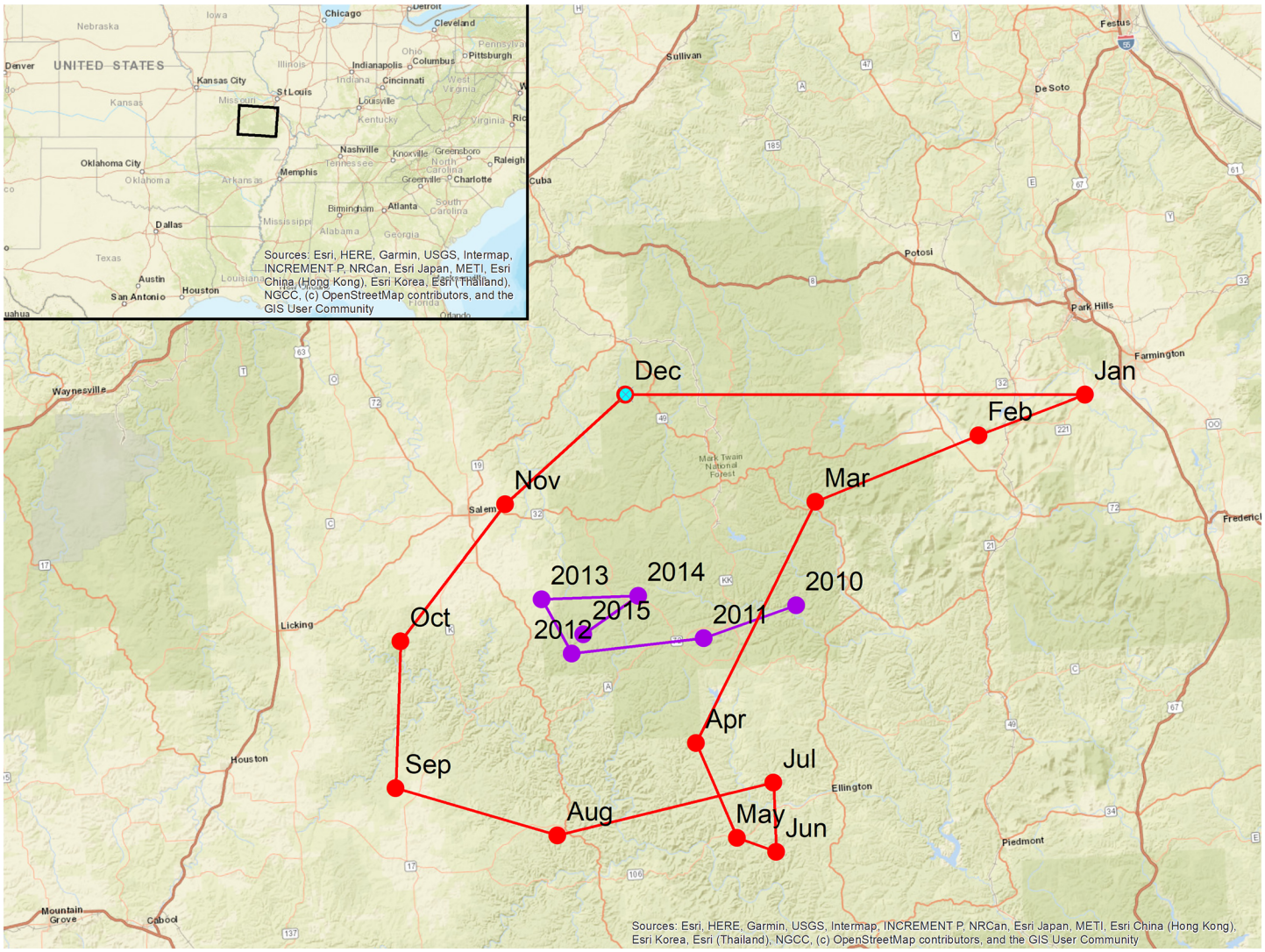

Figure 4. Vulcan v3.0 $FFCO_2$ emissions center of mass estimate. Red line/symbols denote 2010–2015 annual time series. Purple line/symbols denote monthly mean $FFCO_2$ emissions.

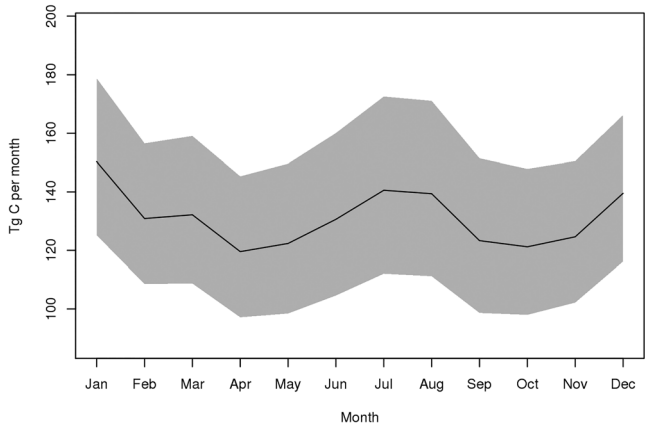

Figure 5. Vulcan v3.0 2011 $FFCO_2$ emissions for the United States by month with 95% confidence interval. Units: TgC/month.

ODIAC2013a output over the U.S. domain in the hope of providing insight into one or both of the emission estimates. First the Vulcan output is gridded to ODIAC grid which, though commonly reported at 1 km × 1 km (e.g., Oda et al., 2018), is actually on a grid dimensioned 30 arcsec × 30 arcsec. This is done by gridding Vulcan directly from its native resolution (points, lines, and polygons) to the 30 arcsec grid. We masked the ODIAC2013a output with a mask that includes all U.S. contiguous land surface gridcells and all gridcells offshore for which Vulcan possesses a non-zero emission value. We estimate the ODIAC emissions to be 1,453.5 TgC/year for the year 2011. The same mask applied to Vulcan results in $FFCO_2$ emissions of 1,553.8 TgC/year (distinct from the unmasked Vulcan total of 1,589.9 TgC/year) or a difference of 1,00.3 MtC/year (7.6%). We also removed all CMV emissions from Vulcan due to the fact that the ODIAC2013a data product does not include any bunker fuels in the emissions. We make no adjustment to the Vulcan airport emissions, though a portion is also likely in the

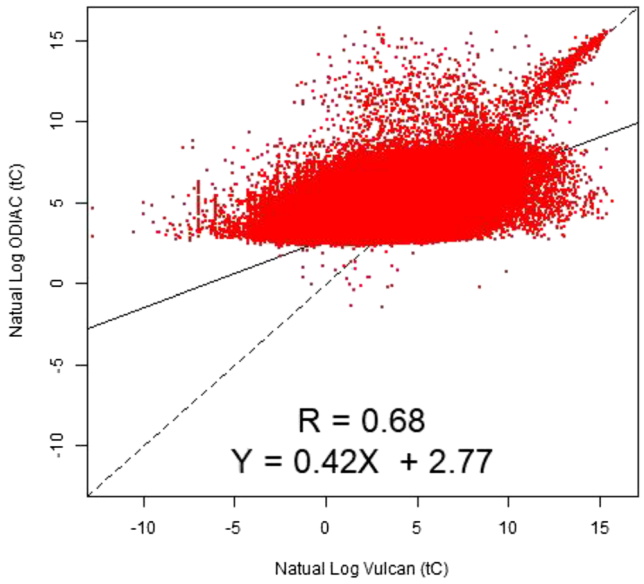

Figure 6. Comparison of log-transformed ODIAC (*y* axis) and Vulcan v3.0 (*x* axis) $FFCO_2$ emissions (units: Natural log tC).

bunker fuel category. The inability to precisely isolate the bunker fuel amounts from Vulcan will result in comparison uncertainties but these are considered small relative to the scale at which the comparison is made. It is worth noting that the ODIAC data product only performs spatialization of the national CDIAC $FFCO_2$ emissions, but because the additional masking is performed, the CDIAC U.S. totals are not directly comparable to the results presented here (Boden et al., 2016).

At the individual gridcell spatial scale, further detail on differences between the two data products can be examined (Figure 6). Three different relationships appear in the log-transformed spatial gridcell comparison with a correlation coefficient of 0.68 and a slope of 0.42 (change in ODIAC/change in Vulcan). The first shows good correlation close to the 1:1 line for large emitting gridcells. These are gridcells dominated by power production facilities and hence, traced to common regulatory data reporting in the two data products. The second relationship evident in the paired gridcell comparison shows rough correspondence whereby Vulcan has a larger range of emission values to a narrower ODIAC range rotated clockwise from the 1:1 line. There is also a well-defined lower threshold of emissions in ODIAC (~20.9 tC/year), likely tied to the threshold associated with low levels of nighttime lighting, a dominant driver of the ODIAC spatial distribution (Gurney, Patarasuk, et al., 2019). The third discrete relationship is a non-correlated collection of paired gridcells in the upper range of ODIAC emissions for which the Vulcan counterparts exhibit midrange emission values.

When presented explicitly in space, total ODIAC and Vulcan $FFCO_2$ emissions show similar spatial patterns at the domain-wide scale, characterized by large concentrations in urban centers across the U.S. landscape, particularly along the Northeastern seaboard and the upper Midwest (Figures 7a and 7c). ODIAC exhibits large numbers of gridcells in rural areas across the Western U.S. with no emission value, likely due to the lack of a nighttime light signal in those areas. This is further demonstrated by the emission histogram (Figures 7b and 7d) whereby ODIAC has a distinct lower cutoff at 13.3 tC/year (natural log of which is 2.59) compared to Vulcan which has a more continuously declining low value distribution. The maximum emission frequency bin for ODIAC is centered at 27.4 tC/year whereas the equivalent value for Vulcan is 9.3 tC/year. Vulcan gridcells in these areas have emission values but they are small in comparison to more populated areas and can be dominated by nonroad emissions which use large spatial proxies for distribution. In estimating the gridcell-scale relative emissions difference (GRD), these pairs are excluded. GRD values are high throughout the populated portions of the United States., particularly in the Eastern half of the country. There are large spatially continuous areas in which ODIAC emissions exceed Vulcan and vice-versa. Large differences occur in urban centers, most notably in the Western United States, with Vulcan often exceeding ODIAC emissions in the urban core but ODIAC exceeding Vulcan outside of the urban core in these cities. (e.g., Phoenix, Dallas, Los Angeles, St Louis).

To provide an average relative difference between the two data products, we calculate the gridcell absolute median relative difference, *GAMRD*, the median of a set of individual paired gridcell relative differences, where the differences are represented in absolute units (i.e., so all GRD values are positive). GAMRD is calculated as,

$$\boldsymbol{GAMRD} = med\left\{\frac{abs\left(E_i^A - E_i^V\right)}{\frac{E_i^A \mp E_i^V}{2}}\right\} \quad (1)$$

where E represented emissions for the ODIAC (A) and Vulcan (V) for each ith paired gridcell. We only include gridcell pairs in which neither of the emission values is zero. We find that the GAMRD between the ODIAC and Vulcan v3.0 $FFCO_2$ emissions at the 1 km × 1 km spatial scale is 100.4%.

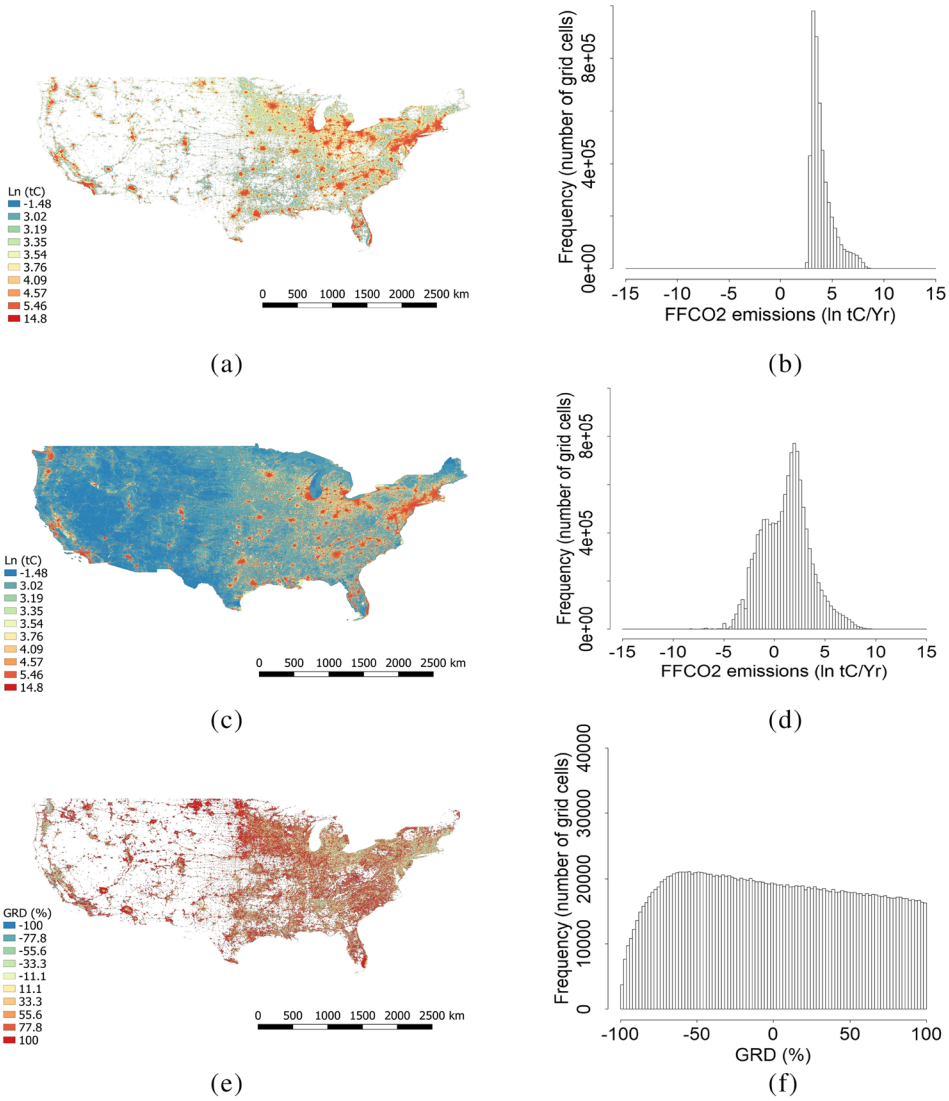

Figure 7. Comparison of the ODIAC and Vulcan total $FFCO_2$ emissions as mapped distributions (left) and frequency histograms (right) for contiguous United States only: (a, b) ODIAC total $FFCO_2$ emissions; (c, d) Vulcan total $FFCO_2$ emissions; (e, f) GRD values ({ODIAC-Vulcan}/Vulcan) (values larger than 99% and smaller than −99% were excluded from the GRD frequency distribution).

The other means by which to assess the Vulcan results is via comparison to recent work using $14CO_2$ measurements and an atmospheric inversion approach by Basu et al. (2020). In that study, the mean of the ensemble of atmospheric CO_2 inversion estimates was within 1.4% of the total U.S. Vulcan estimate in the year 2011.

The increased resolution of the Vulcan v3.0 $FFCO_2$ emissions data product (1 km × 1 km) in comparison to the previous Vulcan v2.0 data product (10 km × 10 km) raises the prospect of supplying information that resolves sub-city spatial scales (e.g., neighborhood) in a comprehensive fashion across the entire U.S. landscape. At this resolution, most urbanized areas in the United States would comprise domains much larger than the 1 km × 1 km resolution and, hence, have sub-domain information emissions content. In this way, the Vulcan v3.0 $FFCO_2$ emissions data product offers a Scope 1, high-resolution inventory estimates for every urbanized area in the United States (Figure 8).

After adopting the U.S. census "urbanized area" boundary definition (https://www.census.gov/programs-surveys/geography/guidance/geo-areas/urban-rural/2010-urban-rural.html), total U.S. $FFCO_2$ emissions

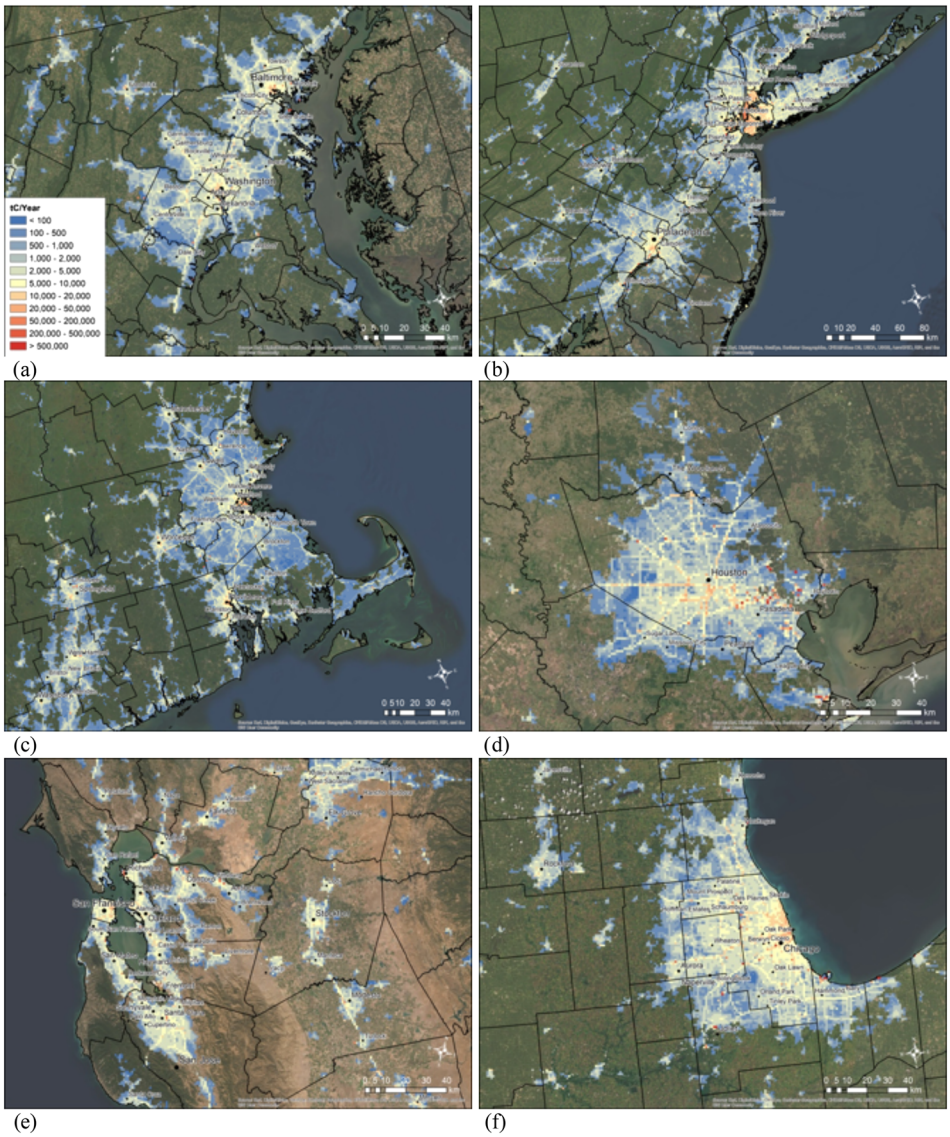

Figure 8. Vulcan v3.0 $FFCO_2$ emissions for a selected group of U.S. urban areas. (a) Washington DC; (b) New York; (c) Boston; (d) Houston; (e) San Francisco; (f) Chicago.

within these urban area boundaries come to 45.1% of the total Vulcan $FFCO_2$ contiguous U.S. emissions in 2011 (710.4 TgC; −13.7%/+16.7%). We narrow urban emissions to the sum of residential, commercial and onroad in an effort to eliminate emissions sectors that are often historically artifactual to location within a given urban area (e.g., power plants, industrial facilities) and hence, less directly related to urban residents and their emitting activities. The sum of these three sectors within the urbanized area boundary accounts for 65% of these same three sectors at the national scale, slightly less than the proportion of the U.S. population within the urbanized area boundary, 73%. This indicates that for the sum of the residential, commercial and onroad sectors, urban residents emit less per capita than non-urban residents in the contiguous United States.

5. Caveats

A number of caveats are worth noting in relation to the Vulcan v3.0 $FFCO_2$ emissions data product. First, the uncertainty estimation remains limited with additional need for errors related to downscaling in both space and time. Additional uncertainty due to these downscaling steps (e.g., from county to U.S. Census

block-group and from annual/monthly to hourly estimates) remains incomplete. Similarly, estimation of space and time error correlations have not been attempted but are useful, particularly for atmospheric inversion applications. Second, independent validation of the Vulcan v3.0 at space/time scales finer than the national/monthly resolution are needed. Finally, the Vulcan Project only includes fossil fuel carbon dioxide. Currently there are no plans to formally estimate additional GHGs, such as methane (CH_4), nitrous oxide (N_2O), or halogenated species. The rationale for focusing on $FFCO_2$ emissions is their amenability to being quantified from a bottom-up approach, difficult to do for other GHGs. However, given the practical utility of having a comprehensive GHG emissions data product at high-resolution for research applications, we are currently incorporating an existing CH_4 emissions data product into a single downloadable result in collaboration with colleagues.

6. Conclusions

Fossil fuel carbon dioxide ($FFCO_2$) emissions, spanning the years 2010–2015, at a spatial scale of 1 km × 1 km and an hourly temporal scale have been completed for the United States under the Vulcan Project. These Vulcan version 3.0 emissions are constructed through a bottom-up approach, gathering and combining data from multiple sources such as CO emissions reporting, direct flux measurements, and traffic monitoring. We describe the complete Vulcan version 3.0 methodology here, sector-by-sector in addition to the methods for uncertainty estimation.

We estimate $FFCO_2$ emissions for the year 2011 of 1,589.9 TgC with a 95% confidence interval of 1,367/1,853 TgC (−14.0%/+16.6%), implying a one-sigma uncertainty of ~ ±8%. The order of the 2011 $FFCO_2$ emitting sectors shows the electricity production sector accounting for the largest share in the Midwest (44%) and South (46%) while onroad emissions account for the largest share in the West (32%) and Northeast (29%). Overall, 2011 $FFCO_2$ emissions are largest in the South (652 TgC), followed by the Midwest (434 TgC), the West (293 TgC), and the Northeast (200 TgC).

We find that per capita $FFCO_2$ emissions are larger in states proportionately dominated by the electricity production and industrial sectors and smaller in states proportionately dominated by onroad and residential/commercial building emissions. The center of mass (CoM) of $FFCO_2$ emissions in the United States are located in the state of Missouri with mean seasonality that extends toward the northeast in the wintertime then moves toward the Southwest in the summer, likely reflecting the seasonal demand for heating and air conditioning. Comparison to ODIAC, a global gridded $FFCO_2$ emissions estimate shows large differences in both total emissions (100.1 TgC for year 2011) and spatial patterns. The spatial correlation (R^2) between the two data products was 0.38 and the mean absolute difference at the individual gridcell scale was 80.04%.

The Vulcan v3.0 $FFCO_2$ emissions data product offers an immediate high-resolution estimate of emissions in every city within the United States, providing a large potential savings of time and effort for cities planning to develop self-reported city inventories. A number of future research activities are planned or underway that extend the application and analysis of the Vulcan v3.0 $FFCO_2$ emissions. First, a Vulcan v4.0 is under construction that will extend the time series to 2019, using additional data sources and data processing approaches. Vulcan v4.0 is expected to be available in mid-2021. Detailed inter-comparisons with other gridded data products that contain overlap with the U.S. domain is planned in addition to a detailed analysis of the differences between the Vulcan results and those reported by the USEPA. Finally, Research associated with comparison to existing self-reported urban inventories and the addition of indirect $FFCO_2$ emissions (Scopes 2 and 3) are underway.

Conflict of Interest

The authors declare that they have no conflict of interest.

Data Availability Statement

The sector-specific Vulcan v3.0 annual gridded emissions data product can be downloaded from the Oak Ridge National Laboratory Distributed Active Archive Center (ORNL DAAC) (https://doi.org/10.3334/ORNLDAAC/1741) and is distributed under Creative Commons Attribution 4.0 International (CC-BY 4.0,

https://creativecommons.org/licenses/by/4.0/deed.en). The Vulcan v3.0 $FFCO_2$ emissions data product is provided in annual 1 km × 1 km NetCDF file formats, one file for each of the 6 years (2010–2015). The annual files vary in size (by sector) with the largest individual file being approximately 50 GB. Separate files are available for Alaska and the contiguous United States (Gurney, Liang, et al., 2019). Attempts will be made to update the Vulcan $FFCO_2$ emissions on an annual basis using the multiyear approach outlined in section 2.1.1.1. Updates availing of new releases of underlying data (e.g., the NEI) will also be attempted at an interval of 2–3 years, depending upon support and timing of updates to the underlying data.

Acknowledgments
This research was made possible through support from the National Aeronautics and Space Administration Grant NNX14AJ20G and the NASA Carbon Monitoring System program, Understanding User Needs for Carbon Information project (Subcontract 1491755).

References

Andres, R. J., Boden, T. A., Bréon, F., Ciais, P., Davis, S., Erickson, D., et al. (2012). A synthesis of carbon dioxide emissions from fossil-fuel combustion. *Biogeosciences Discussions*, *9*(1), 1299–1376. https://doi.org/10.5194/bgd-9-1299-2012

Andres, R. J., Fielding, D. J., Marland, G., Boden, T. A., Kumar, N., & Kearney, A. T. (1999). Carbon dioxide emissions from fossil fuel use, 1751-1950. *Tellus Series B: Chemical and Physical Meteorology*, *51*(4), 759–765. https://doi.org/10.1034/j.1600-0889.1999.t01-3-00002.x

Andres, R. J., Marland, G., Fung, I., & Matthews, E. (1996). A 1° × 1° distribution of carbon dioxide emissions from fossil fuel consumption and cement manufacture, 1950–1990. *Global Biogeochemical Cycles*, *10*(3), 419–429. https://doi.org/10.1029/96GB01523

Andrew, R. M. (2018). Global CO_2 emissions from cement production. *Earth System Science Data*, *10*(1), 195–217. https://doi.org/10.5194/essd-10-195-2018

Asefi-Najafabady, S., Rayner, P. J., Gurney, K. R., McRobert, A., Song, Y., Coltin, K., et al. (2014). A multiyear, global gridded fossil fuel CO2 emission data product: Evaluation and analysis of results. *Journal of Geophysical Research: Atmospheres*, *119*, 10,213–10,231. https://doi.org/10.1002/2013JD021296

Baldasano, J. M., Güereca, L. P., López, E., Gassó, S., & Jimenez-Guerrero, P. (2008). Development of a high-resolution (1 km × 1 km, 1 h) emission model for Spain: The High-Elective Resolution Modelling Emission System (HERMES). *Atmospheric Environment*, *42*(31), 7215–7233. https://doi.org/10.1016/j.atmosenv.2008.07.026

Basu, S., Lehman, S. J., Miller, J. B., Andrews, A. E., Sweeney, C., Gurney, K. R., & Tans, P. P. (2020). Constraints on Fossil Fuel CO_2 Emissions from Measurements of 14C in Atmospheric CO_2. *Proceedings of the National Academy of Sciences of the United States of America*, accepted, *117*(24), 13,300–13,307. https://doi.org/10.1073/pnas.1919032117

Boden, T. A., Marland, G., & Andres, R. J. (2016). *Global, Re- gional, and National Fossil-Fuel CO_2 Emissions*. Oak Ridge, Tenn., USA: Carbon Dioxide Information Analysis Center, Oak Ridge National Labo- ratory, U.S. Department of Energy. https://doi.org/10.3334/CDIAC/00001_V2016

Bun, R., Gusti, M., Kujii, L., Tokar, O., Tsybrivskyy, Y., & Bun, A. (2007). Spatial GHG inventory: Analysis of uncertainty sources. A case study for Ukraine. In D. Lieberman, M. Jonas, Z. Nahorski, & S. Nilsson (Eds.), *Accounting for climate change* (pp. 63–74). Dordrecht: Springer. https://doi.org/10.1007/978-1-4020-5930-8_6

Bun, R., Nahorski, Z., Horabik-Pyzel, J., Danylo, O., See, L., Charkovska, N., et al. (2018). Development of a high-resolution spatial inventory of greenhouse gas emissions for Poland from stationary and mobile sources. *Mitigation and Adaptation Strategies for Global Change*, *24*(6), 853–880. https://doi.org/10.1007/s11027-018-9791-2

Cai, B., Liang, S., Zhou, J., Wang, J., Cao, L., Qu, S., et al. (2018). China high resolution emission database (CHRED) with point emission sources, gridded emission data, and supplementary socioeconomic data. *Resources, Conservation and Recycling*, *129*, 232–239. https://doi.org/10.1016/j.resconrec.2017.10.036

California Air Resources Board (2014). EMFAC2014 volume I—User's guide, v1.0.7, April 30, 2014, California Environmental Protection Agency Air Resources Board, Mobile Source Analysis Branch, Air Quality Planning & Science Division.

California Air Resources Board (2015). EMFAC2014 volume III—Technical documentation (Publication v1.0.7, CARB, 2015). Retrieved from https://www.arb.ca.gov/emfac/2014/

Charkovska, N., Halushchak, H., Bun, R., Nahorski, Z., Oda, T., Jonas, M., & Topylko, P. (2019). A high-definition spatially explicit modelling approach for national greenhouse gas emissions from industrial processes: reducing errors and uncertainties in global emissions modelling. *Mitigation and Adaptation Strategies for Global Change*, *24*(6), 907–939. https://doi.org/10.1007/s11027-018-9836-6

Code of Federal Regulations (2008). Protection of Environment, Environmental Protection Agency, 40 CFR Part 75, Continuous emission monitoring, Code of Federal Regulations, Revised as of January 24, 2008. https://www.ecfr.gov/cgi-bin/text-idx?SID=4719db7a48cd26050b0732d0f9adc3ad&mc=true&node=pt40.2.51&rgn=div5. AERR summary: https://www.epa.gov/air-emissions-inventories/air-emissions-reporting-requirements-aerr#rule-summary

Commercial Building Energy Consumption Survey (2016). 2012 CBECS microdata files and information, U.S. Energy Information Administration. Data retrieved from: https://www.eia.gov/consumption/commercial/data/2012/index.php?view=microdata (Aug 1, 2018).

Cooke, W. F., Liousse, C., Cachier, H., & Feichter, J. (1999). Construction of a 1° × 1° fossil fuel emission data set for carbonacious aerosol and implementation and radiative impact in the ECHAM4 model. *Journal of Geophysical Research*, *104*(D18), 22,137–22,162. https://doi.org/10.1029/1999JD900187

Danylo, O., Bun, R., See, L., & Charkovska, N. (2019). High-resolution spatial distribution of greenhouse gas emissions in the residential sector. *Mitigation and Adaptation Strategies for Global Change*, *24*(6), 941–967. https://link.springer.com/article/, https://doi.org/10.1007/s11027-019-9846-z

Davis, S. J., & Caldeira, K. (2010). Consumption-based accounting of CO_2 emissions. *Proceedings of the National Academy of Sciences of the United States of America*, *107*(12), 5687–5692. https://doi.org/10.1073/pnas.0906974107

Denier van der Gon, H. A. C., Kuenen, J. J. P., Janssens-Maenhout, G., Döring, U., Jonkers, S., & Visschedijk, A. (2017). TNO_CAMS high resolution European emission inventory 2000–2014 for anthropogenic CO_2 and future years following two different pathways. *Earth System Science Data Discussions*, 1–30. https://doi.org/10.5194/essd-2017-124

Department of Energy/Energy Information Administration (2003). Electric power monthly March 2003, Energy Information Administration, Office of Coal, Nuclear, and Alternate Fuels, U.S. Department of Energy, Washington D.C. 20585, DOE/EIA-0226 (2003/03).

Department of Energy/Energy Information Administration (2011). Electric power annual 2010, November 2011, Retrieved from http://www.eia.gov/cneaf/electricity/epa/epa_sum.html

Department of Energy/Energy Information Administration (2018). State energy consumption estimates 1960 through 2016, DOE/EIA-0214(2016), June 2018, Washington DC.

Durant, A. J., LeQuere, C., Hope, C., & Friend, A. D. (2011). Economic value of improved quantification in global sources and sinks of carbon dioxide. *Philosophical Transactions of the Royal Society A*, *369*(1943), 1967–1979. https://doi.org/10.1098/rsta.2011.0002

Eastern Research Group (2011). Documentation for locomotive component of the national emissions inventory methodology, prepared by: Eastern Research Group, ERG No.: 0245.02.401.001, Contract No.: EP-D-07-097, 2011.

Eastern Research Group (2012). Development of 2011 railroad component for national emissions inventory, Memorandum from Heather Perez, Susan McClutchey, and Richard Billings/ERG, to Laurel Driver/US EPA, September 5, 2012

Eastern Research Group, Inc. (2001). Introduction to area source emissions inventory development, Volume III, Chapter 1, prepared for: Area Sources Committee, Emission Inventory Improvement Program, January 2001.

Federal Emergency Management Agency (2017). HAZUS database. Retreived from https://www.fema.gov/summary-databases-hazus-multi-hazard (Aug 1, 2018).

Federal Highway Administration (2014). Highway performance monitoring system: Field manual, Office of Highway Policy Information, Office of Management & budget (OMB) Control No. 2125–0028, March 2014. Retrieved from https://www.fhwa.dot.gov/policyinformation/hpms/shapefiles.cfm

Gately, C. K., & Hutyra, L. R. (2017). Large uncertainties in urban-scale carbon emissions. *Journal of Geophysical Research: Atmospheres*, *122*, 11,242–11,260. https://doi.org/10.1002/2017JD027359

Gately, C. K., Hutyra, L. R., Wing, I. S., & Brondfield, M. N. (2013). A bottom up approach to on-road CO_2 emissions estimates: Improved spatial accuracy and applications for regional planning. *Environmental Science & Technology*, *47*(5), 2423–2430. https://doi.org/10.1021/es304238v

Gaubert, B., Stephens, B. B., Basu, S., Chevallier, F., Deng, F., Kort, E. A., et al. (2019). Global atmospheric CO_2 inverse models converging on neutral tropical land exchange but disagreeing on fossil fuel and atmospheric growth rate. *Biogeosciences*, *16*(1), 117–134. https://doi.org/10.5194/bg-16-117-2019

Ghosh, T., Elvidge, C. D., Sutton, P. C., Baugh, K. E., Ziskin, D., & Tuttle, B. T. (2010). Creating a global grid of distributed fossil fuel CO_2 emissions from nighttime satellite imagery. *Energies*, *3*(12), 1895–1913. https://doi.org/10.3390/en3121895

Gregg, J. S., & Andres, R. J. (2008). A method for estimating the temporal and spatial patterns of carbon dioxide emissions from national fossil-fuel consumption. *Tellus Series B: Chemical and Physical Meteorology*, *60 B*(1), 1–10. https://doi.org/10.1111/j.1600-0889.2007.00319.x

Gregg, J. S., Losey, L. M., Andres, R. J., Blasing, T. J., & Marland, G. (2009). The temporal and spatial distribution of carbon dioxide emissions from fossil-fuel use in North America. *Journal of Applied Meteorology and Climatology*, *48*(12), 2528–2542. https://doi.org/10.1175/2009JAMC2115.1

Gurney, K. R., Chen, Y. H., Maki, T., Kawa, S. R., Andrews, A., & Zhu, Z. (2005). Sensitivity of atmospheric CO_2 inversions to seasonal and interannual variations in fossil fuel emissions. *Journal of Geophysical Research*, *110*, D10308. https://doi.org/10.1029/2004JD005373

Gurney, K. R., Huang, J., & Coltin, K. (2016). Bias present in US federal agency power plant CO_2 emissions data and implications for the US clean power plan. *Environmental Research Letters*, *11*, 064005. https://doi.org/10.1088/1748-9326/11/6/064005

Gurney, K. R., Law, R. M., Denning, A. S., Rayner, P. J., Baker, D., Bousquet, P., et al. (2002). Towards robust regional estimates of CO_2 sources and sinks using atmospheric transport models. *Nature*, *415*(6872), 626–630. https://doi.org/10.1038/415626a

Gurney, K. R., Liang, J., O'Keeffe, D. O., Patarasuk, R., Hutchins, M., Huang, J., et al. (2018). Comparison of global downscaled versus bottom-up fossil fuel CO_2 emissions at the urban scale in four US urban areas. *Journal of Geophysical Research: Atmospheres*, *124*, 2823–2840. https://doi.org/10.1029/2018JD028859

Gurney, K. R., Liang, J., Patarasuk, R., Song, Y., Huang, J., & Roest, G. (2019). Vulcan fossil fuel carbon dioxide ($FFCO_2$) emissions data product, version 3.0, 1 km grid. https://doi.org/10.3334/ORNLDAAC/1741

Gurney, K. R., Mendoza, D., Zhou, Y., Fischer, M., de la Rue du Can, S., Geethakumar, S., & Miller, C. (2009). The Vulcan project: High resolution fossil fuel combustion CO_2 emissions fluxes for the United States. *Environmental Science & Technology*, *43*(14), 5535–5541. https://doi.org/10.1021/es900806c

Gurney, K. R., Patarasuk, R., Liang, J., O'Keeffe, D., Rao, P., & Song, Y. (2019). The Hestia fossil fuel CO_2 emissions dataset for the Los Angeles Basin. *Earth System Science Data*, *11*, 1309–1335. https://doi.org/10.5194/essd-11-1309-2019

Gurney, K. R., Razlivanov, I., Song, Y., Zhou, Y., Benes, B., & Abdul-Massih, M. (2012). Quantification of fossil fuel CO_2 emissions on the building/street scale for a large U.S. city. *Environmental Science and Technology*, *46*(21), 12,194–12,202. https://doi.org/10.1021/es3011282

Gurney, K. R., Romero-Lankao, P., Seto, K., Kennedy, C., Grimm, N., Ehleringer, J., et al. (2015). Climate change: Track urban emissions on a human scale. *Nature* (*Comment*, *525*, 179–181 (10 September 2015. https://doi.org/10.1038/525179a

Highway Performance Monitoring System (2017). https://catalog.data.gov/dataset/highway-performance-monitoring-system-hpms-national

Hirsch, J., &Associates (2004). Energy simulation training for design & construction professionals. Retrieved from: http://doe2.com/download/equest/eQuestTrainingWorkbook.pdf (Aug 1, 2018). eQuest model download available from: http://www.doe2.com/eQuest/ (Aug 1, 2018).

Hoesly, R. M., Smith, S. J., Feng, L., Klimont, Z., Janssens-Maenhout, G., Pitkanen, T., et al. (2018). Historical (1750-2014) anthropogenic emissions of reactive gases and aerosols from the community emissions data System (CEDS). *Geoscientific Model Development*, *11*(1), 369–408. https://doi.org/10.5194/gmd-11-369-2018

Intergovernmental Panel on Climate Change (2006). "IPCC guidelines for national greenhouse gas inventories, prepared by the National Greenhouse Gas Inventories Programme" (IGES, Japan, 2006).

Intergovernmental Panel on Climate Change (2013). Working group i contribution to the IPCC fifth assessment report, climate change 2013: The physical science basis.

IPCC (2018). Special report on 1.5 degrees: Summary for policymakers. Retrieved from https://www.ipcc.ch/site/assets/uploads/sites/2/2019/05/SR15_SPM_version_report_LR.pdf

Ivanova, D., Vita, G., Steen-Olsen, K., Stadler, K., Melo, P. C., Wood, R., & Hertwich, E. G. (2017). Mapping the carbon footprint of EU regions. *Environmental Research Letters*, *12*, 054013. https://doi.org/10.1088/1748-9326/aa6da9

Jannsens-Maenhout, G., Crippa, M., Guizzardi, D., Muntean, M., Schaaf, E., Dentener, F., et al. (2019). EDGAR v4.3.2 Global Atlas of the three major greenhouse gas emissions for the period 1970–2012. *Earth System Science Data*, *11*, 959–1002. https://doi.org/10.5194/essd-11-959-2019

Janssens-Maenhout, G., Petrescu, A. M. R., Muntean, M., & Blujdea, V. (2013). Verifying greenhouse gas emissions: Methods to support international climate agreements. *Greenhouse Gas Measurement and Management*, *1*(2), 132–133. https://doi.org/10.1080/20430779.2011.579358

Jones, C., & Kammen, D. M. (2014). Spatial distribution of U.S. household carbon footprints reveals suburbanization undermines greenhouse gas benefits of urban population density. *Environmental Science & Technology*, *48*(2), 895–902. https://doi.org/10.1021/es4034364

Jones, C. M., & Kammen, D. M. (2011). Quantifying carbon footprint reduction opportunities for U.S. households and communities. *Environmental Science and Technology*, *45*(9), 4088–4095. https://doi.org/10.1021/es102221h

Keeling, C. D. (1973). The production of carbon dioxide from fossil fuels and limestone. *Tellus*, *25*(2), 174–198.

Kurokawa, J., Ohara, T., Morikawa, T., Hanayama, S., Janssens-Maenhout, G., Fukui, T., et al. (2013). Emissions of air pollutants and greenhouse gases over Asian regions during 2000–2008: Regional Emission inventory in ASia (REAS) version 2. *Atmospheric Chemistry and Physics*, *13*(21), 11,019–11,058. https://doi.org/10.5194/acp-13-11019-2013

LandScan Geographic Information Science & Technology, Oak Ridge National Laboratoryhttps://landscan.ornl.gov/

Lauvaux, T., Gurney, K. R., Miles, N. L., Davis, K. J., Richardson, S. J., Deng, A., et al. (2020). Policy-relevant assessment of urban greenhouse gas emissions. *Environmental Science & Technology*, *54*(16), 10,237–10,245. https://doi.org/10.1021/acs.est.0c00343

LeQuéré, C., Andrew, R., Friedlingstein, P., Sitch, S., Hauck, J., Pongratz, J., et al. (2018). Global carbon budget 2018. *Earth System Science Data*, *10*(4), 2141–2194. https://doi.org/10.5194/essd-10-2141-2018

Liu, F., Zhang, Q., Tong, D., Zheng, B., Li, M., Huo, H., & He, K. B. (2015). High-resolution inventory of technologies, activities, and emissions of coal-fired power plants in China from 1990 to 2010. *Atmospheric Chemistry and Physics*, *15*(23), 13,299–13,317. https://doi.org/10.5194/acp-15-13299-2015

Macknick, J. (2011). Energy and CO_2 emission data uncertainties. *Carbon Management*, *2*(2), 189–205. https://doi.org/10.4155/cmt.11.10

Manufacturing Energy Consumption Survey (2010). 2010 MECS survey data, U.S. Energy Information Administration. Retrieved from https://www.eia.gov/consumption/manufacturing/data/2010/#r10 (Aug 1, 2018).

Marion, W., & Urban, K. (1995). User's manual for TMY2s Typical Meteorological Years. National Renewable Energy Laboratory (NREL), Under Contract No. DE-AC36-83CH10093, June 1995.

Marland, G., Rotty, R. M., & Treat, N. L. (1985). CO_2 from fossil fuel burning: Global distribution of emissions. *Tellus B*, *37*(4–5), 243–258. https://doi.org/10.3402/tellusb.v37i4-5.15028

Mendoza, D., Gurney, K. R., Geethakumar, S., Chandrasekaran, V., Zhou, Y., & Razlivanov, I. (2013). Implications of uncertainty on regional CO_2 mitigation policies for the U.S. onroad sector based on a high-resolution emissions estimate. *Energy Policy*, *55*, 386–395. https://doi.org/10.1016/j.enpol.2012.12.027

Minx, J., Baiocchi, G., Wiedmann, T., Barrett, J., Creutzig, F., Feng, K., et al. (2013). Carbon footprints of cities and other human settlements in the UK. *Environmental Research Letters*, *8*, 035039. https://doi.org/10.1088/1748-9326/8/3/035039

Moran, D., Kanemoto, K., Jiborn, M., Wood, R., Többen, J., & Seto, K. C. (2018). Carbon footprints of 13 000 cities. *Environmental Research Letters*, *13*, 064041. https://doi.org/10.1088/1748-9326/aac72a

National Research Council (2010). *Verifying Greenhouse Gas Emissions: Methods to Support International Climate Agreements*. Washington DC: The National Academies Press. https://doi.org/10.17226/12883

Oda, T., & Maksyutov, S. (2011). A very high-resolution (1km×1 km) global fossil fuel CO2 emission inventory derived using a point source database and satellite observations of nighttime lights. *Atmospheric Chemistry and Physics*, *11*(2), 543–556. https://doi.org/10.5194/acp-11-543-2011

Oda, T., Maksyutov, S., & Andres, R. J. (2018). The Open-source Data Inventory for Anthropogenic CO_2, version 2016 (ODIAC2016): A global monthly fossil fuel CO_2 gridded emissions data product for tracer transport simulations and surface flux inversions. *Earth System Science Data*, *10*(1), 87–107. https://doi.org/10.5194/essd-10-87-2018

Ohara, T., Akimoto, H., Kurokawa, J., Horii, N., Yamaji, K., Yan, X., et al. (2007). An Asian emission inventory of anthropogenic emission sources for the period 1980–2020 To cite this version: and Physics An Asian emission inventory of anthropogenic emission sources for the period 1980–2020. *Atmospheric Chemistry and Physics*, *7*(16), 4419–4444. https://doi.org/10.5194/acp-7-4419-2007

Olivier, J. G. J., Bloos, J. P. J., Berdowski, J. J. M., Visschedijk, A. J. H., & Bouwman, A. F. (1999). A 1990 global emission inventory of anthropogenic sources of carbon monoxide on 1° × 1° developed in the framework of EDGAR/GEIA. *Chemosphere - Global Change Science*, *1*(1–3), 1–17. https://doi.org/10.1016/S1465-9972(99)00019-7

Olivier, J. G. J., Van Aardenne, J. A., Dentener, F. J., Pagliari, V., Ganzeveld, L. N., & Peters, J. A. H. W. (2005). Recent trends in global greenhouse gas emissions: regional trends 1970–2000 and spatial distribution of key sources in 2000. *Environmental Sciences*, *2*(2–3), 81–99. https://doi.org/10.1080/15693430500400345

Ou, J., Liu, X., Li, X., Li, M., & Li, W. (2015). Evaluation of NPP-VIIRS nighttime light data for mapping global fossil fuel combustion CO_2 emissions: A comparison with DMSP-OLS nighttime light data. *PLoS ONE*, *10*(9), e0138310. https://doi.org/10.1371/journal.pone.0138310

Patarasuk, R., Gurney, K. R., O'Keeffe, D., Song, Y., Huang, J., Rao, P., et al. (2016). Urban high-resolution fossil fuel CO_2 emissions quantification and exploration of emission drivers for potential policy applications. *Urban Ecosystem*, *19*(3), 1013–1039. https://doi.org/10.1007/s11252-016-0553-1

Petron, G., Tans, P., Frost, G., Chao, D., & Trainer, M. (2008). High resolution emissions of CO_2 from power generation in the USA. *Journal of Geophysical Research*, *113*, 1–9. https://doi.org/10.1029/2007/JG000602

Peylin, P., Houweling, S., Krol, M. C., Karstens, U., Rödenbeck, C., Geels, C., et al. (2011). Importance of fossil fuel emission uncertainties over Europe for CO_2 modeling: Model intercomparison. *Atmospheric Chemistry and Physics*, *11*(13), 6607–6622. https://doi.org/10.5194/acp-11-6607-2011

Pincetl, S., Chester, M., Circella, G., Fraser, A., Mini, C., Murphy, S., et al. (2014). Enabling future sustainability transitions: An urban metabolism approach to Los Angeles. *Journal of Industrial Ecology*, *18*(6), 871–882. https://doi.org/10.1111/jiec.12144

Portland Cement Company, Economic Research Department (2006). *U.S. and Canadian Portland Cement Industry Plant Information Summary*. Skokie, IL: Portland Cement Association.

Quick, J. C. (2010). Carbon dioxide emission factors for U.S. coal by origin and destination. *Environmental Science and Technology*, *44*(7), 2709–2714. https://doi.org/10.1021/es9027259

Rayner, P. J., Raupach, M. R., Paget, M., Peylin, P., & Koffi, E. (2010). A new global gridded data set of CO_2 emissions from fossil fuel combustion: Methodology and evaluation. *Journal of Geophysical Research*, *115*, 1–11. https://doi.org/10.1029/2009JD013439

Residential Energy Consumption Survey (2013). 2009 RECS survey data, U.S. Energy Information Administration. Retrieved from https://www.eia.gov/consumption/residential/data/2009/index.php?view=microdata (Aug 1, 2018).

Shu, Y., & Lam Nina, N. S. N. (2011). Spatial disaggregation of carbon dioxide emissions from road traffic based on multiple linear regression model. *Atmospheric Environment*, *45*(3), 634–640. https://doi.org/10.1016/j.atmosenv.2010.10.037

U.S. Environmental Protection Agency (2012). Motor vehicle emission simulator (MOVES): User guide for MOVES2010b Office of Transportation and Air Quality, EPA-420-B-12-001b. Retrieved from https://nepis.epa.gov/Exe/ZyPDF.cgi?Dockey=P100EP28.pdf (August 12, 2018).

United States Environmental Protection Agency (1995). fire version 5.0 source classification codes and emission factor listing for criteria air pollutants, Office of Air Quality Planning and Standards, Research Triangle Park, NC 27711, EPA-454/R-95-012, August 1995.

United States Environmental Protection Agency (2005a). Emissions inventory guidance for implementation of ozone and particulate matter national ambient air quality standards (NAAQS and regional haze regulations), Emissions Inventory Group, Emissions, Monitoring and Analysis Division, Office of Air Quality Planning and Standards, U.S. Environmental Protection Agency, Research Triangle Park, NC 27711, EPA-454/R-05-001, August.

United States Environmental Protection Agency (2005b). Plain english guide to the part 75 rule, U.S. Environmental Protection Agency, Clean Air Markets Division.

United States Environmental Protection Agency (2005c). EPA's national mobile inventory model (NMIM), A consolidated emissions modeling system for MOBILE6 and NONROAD, Office of Transportation and Air Quality, Assessment and Standards Division, U.S. Environmental Protection Agency, EPA420-R-05-024, December.

United States Environmental Protection Agency (2005d). User's guide for the final NONROAD2005 model, assessment and standards, Division Office of Transportation and Air Quality U.S. Environmental Protection Agency, December.

United States Environmental Protection Agency (2010). Draft part 75 emissions monitoring policy manual, U.S. Environmental Protection Agency, Clean Air Markets Division, Washington, D.C., April 2010.

United States Environmental Protection Agency (2011). 2011 national emissions inventory, version 1 technical support document, June 2014 – Draft. Office of Air Quality Planning and Standards. Retrieved from https://www.epa.gov/air-emissions-inventories/2011-national-emissions-inventory-nei-technical-support-document (August 12, 2018).

United States Environmental Protection Agency (2015a). 2011 national emissions inventory, version 2 Technical Support Document, U.S. Environmental Protection Agency, Office of Air Quality Planning and Standards, Air Quality Assessment Division, Emissions Inventory and Analysis Group, Research Triangle Park, North Carolina, August 2015. Retrieved from www.epa.gov/air-emissions-inventories/2011-national-emissions-inventory-nei-data

United States Environmental Protection Agency (2015b). 40 DFR part 60, EPA-HQ-OAR-2013-0602; FRL-XXXX-XX-OAR, RIN 2060-AR33, carbon pollution emission guidelines for existing stationary sources: Electric utility generating units, August 3, 2015.

United States Environmental Protection Agency (2015c). Technical support document (TSD) preparation of emissions inventories for the version 6.2, 2011 emissions modeling platform, U.S. Environmental Protection Agency, Office of Air Quality Planning and Standards, Air Quality Assessment Division, contacts: Alison Eyth, Jeff Vukovich, August 2015. Retrieved from https://www.epa.gov/air-emissions-modeling/2011-version-62-technical-support-document (July 27, 2018).

United States Environmental Protection Agency (2017). Inventory of U.S. greenhouse gas emissions and sinks 1990–2015, EPA 430-P-17-001.

United States Geological Survey (2013). 2011 minerals yearbook: Cement, U.S. Department of the Interior, U.S. Geological Survey. December 2013.

USGCRP (2018). In N. Cavallaro, G. Shrestha, R. Birdsey, M. A. Mayes, R. G. Najjar, S. C. Reed, P. Romero-Lankao, & Z. Zhu (Eds.), *Second state of the carbon cycle report (SOCCR2): A sustained assessment report* (p. 878). Washington, DC, USA: U.S. Global Change Research Program. https://doi.org/10.7930/SOCCR2.2018

VandeWeghe, J. R., & Kennedy, C. (2007). A spatial analysis of residential greenhouse gas emissions in the Toronto census metropolitan area. *Journal of Industrial Ecology*, *11*(2), 133–144. https://doi.org/10.1162/jie.2007.1220

Wang, J., Cai, B., Zhang, L., Cao, D., Liu, L., Zhou, Y., et al. (2014). High resolution carbon dioxide emission gridded data for China derived from point sources. *Environmental Science and Technology*, *48*(12), 7085–7093. https://doi.org/10.1021/es405369r

Wang, R., Tao, S., Ciais, P., Shen, H. Z., Huang, Y., Chen, H., et al. (2013). High-resolution mapping of combustion processes and implications for CO_2 emissions. *Atmospheric Chemistry and Physics*, *13*(10), 5189–5203. https://doi.org/10.5194/acp-13-5189-2013

Wilson, J., Spinney, J., Millward, H., Scott, D., Hayden, A., & Tyedmers, P. (2013). Blame the exurbs, not the suburbs: Exploring the distribution of greenhouse gas emissions within a city region. *Energy Policy*, *62*, 1329–1335. https://doi.org/10.1016/j.enpol.2013.07.012

Yadav, V., Michalak, A. M., Ray, J., & Shiga, Y. P. (2016). A statistical approach for isolating fossil fuel emissions in atmospheric inverse problems. *Journal of Geophysical Research: Atmospheres*, *121*, 12,490–12,504. https://doi.org/10.1002/2016JD025642

Zhang, Y., Wang, H., Liang, S., Xu, M., Liu, W., Li, S., et al. (2014). Temporal and spatial variations in consumption-based carbon dioxide emissions in China. *Renewable and Sustainable Energy Reviews*, *40*, 60–68. https://doi.org/10.1016/j.rser.2014.07.178

Zheng, B., Huo, H., Zhang, Q., Yao, Z. L., Wang, X. T., Yang, X. F., et al. (2014). High-resolution mapping of vehicle emissions in China in 2008. *Atmospheric Chemistry and Physics*, *14*(18), 9787–9805. https://doi.org/10.5194/acp-14-9787-2014

Zhou, Y., & Gurney, K. R. (2011). Spatial relationships of sector-specific fossil fuel CO_2 emissions in the United States. *Global Biogeochemical Cycles*, *25*, GB3002. https://doi.org/10.1029/2010GB003822

References From the Supporting Information

American Petroleum Institute (2009) Compendium of greenhouse gas emissions methodologies for the oil and natural gas industry, august 2009, American Petroleum Institute, Washington DC 20005.

Federal Highway Administration, & Highway Statistics Series (2011). Highway statistics 2011, User's guide, policy and government affairs, Office of Highway Policy Information. Available at: https://www.fhwa.dot.gov/policyinformation/statistics/2011/userguide.cfm

Federal Highway Administration, & Highway statistics series (2013). Highway Statistics 2013, User's Guide, Policy and Government Affairs, Office of Highway Policy Information. Available at: https://www.fhwa.dot.gov/policyinformation/statistics/2013/userguide.cfm

United States Environmental Protection Agency (2007). Inventory of U.S. greenhouse gas emissions and sinks 1990–2005, EPA 430-R-07-002, April 2007.

United States Environmental Protection Agency (2018). Inventory of U.S. greenhouse gas emissions and sinks 1990–2016, EPA 430-R-18-003.